ROTOR BLADE RADAR ANTENNA

PHASE II

INTERIM TECHNICAL REPORT
NO. 299-099-275

462744

BELL HELICOPTER COMPANY
FORT WORTH, TEXAS
DIVISION OF BELL AEROSPACE CORPORATION • A textron COMPANY

BELL HELICOPTER COMPANY
POST OFFICE BOX 482 • FORT WORTH 1 TEXAS
A DIVISION OF BELL AEROSPACE CORPORATION A textron COMPANY

JANAIR

JOINT ARMY-NAVY AIRCRAFT INSTRUMENTATION RESEARCH

ROTOR BLADE RADAR ANTENNA REPORT
PHASE II

Interim Technical Report

299-099-275

February 1965

By

James E. Palmer
Project Engineer

David W. Young
David W. Young of
David W. Young and Associates, Inc.

APPROVED:

H. W. Upton
Chief Electronics Research Engineer

H. W. Mitchell
Chief Electronics Engineer

OFFICE OF NAVAL RESEARCH
Contract Nonr 4148(00)

This report presents work which was performed under the Joint Army-Navy Aircraft Instrumentation Research (JANAIR) Project, a research and development program directed by the United States Navy, Office of Naval Research. Special guidance is provided to the program for the Army Material Command, the Office of Naval Research and the Bureau of Naval Weapons through an organization known as the JANAIR Committee. The Committee is currently composed of the following representatives:

U. S. Navy, Office of Naval Research
CAPT J. D. Kuser

U. S. Navy, Bureau of Naval Weapons
CDR W. A. Engdahl

U. S. Army, Material Command
Mr. Len Evenson

The goals of JANAIR are:

a. The Joint Army-Navy Aircraft Instrumentation Research (JANAIR) Project, is a research project, the objective of which is to improve the state of the art of piloted aircraft instrumentation.

b. The JANAIR Project is to be responsive to specific problems assigned, and shall provide guidance for aircraft instrumentation research and development programs.

c. The JANAIR Project will conduct feasibility studies and develop concepts in support of service requirements.

d. These efforts shall result in reports and the knowledge to form the basis for development of improved instrumentation systems, components, and subsystems.

ABSTRACT

This report covers a research project administered under the JANAIR Program to investigate the feasibility of using the main rotor blade of a helicopter as a high resolution radar antenna. The purpose of this program conducted by Bell Helicopter Company with David W. Young and Associates, Inc. as a major subcontractor was to refine the design developed under Phase I of Contract Number Nonr 4148(00), documented in Bell Helicopter Company Report No. 299-099-251. Fifteen-inch antenna sections were built and tested to study detailed leading and trailing edge array element environments. A full length, 173-inch array was built and tested. A jig was constructed to accept the full length array, and radiation pattern measurements made of beamwidth, focus, sidelobe levels, and front-to-back ratios. Beamwidth and sidelobes were measured under deflections simulating maximum flight loads. Photographs of thin radar sector slices emphasizing elevation and azimuth obstacle sensing capabilities taken from a modified PPI were compared with optical photographs. The array was then installed, covered with an erosion boot and tested in the leading edge of a used UH-1B rotor blade.

TABLE OF CONTENTS

LIST OF ILLUSTRATIONS

LIST OF ILLUSTRATIONS (Cont'd)

LIST OF ILLUSTRATIONS (Cont'd)

I. INTRODUCTION

This is a JANAIR (Joint Army-Navy Aircraft Instrumentation Research) radar sensor project. The purpose of the project is evaluation of the helicopter rotor blade antenna feasibility through use of a modified Bell Helicopter Company UH-1B helicopter rotor blade (20 feet long) and the David W. Young and Associates, Inc. K_u band cutoff element array antenna (15 feet long).

During the previous contractual phase of the Helicopter Rotor Blade Antenna Research Program (Reference 1), longitudinal resonant slots, with phase reversal were cut in the broad face of the K_q waveguide, used as a transmission line for the K_u band array. A new method of element radiation (other than slots) was attempted to further reduce the height of the vertical cross section for particular application to the leading edge of the blade and to increase the bandwidth of the array. Holes in the cutoff mode were used as the radiating elements for the first time as part of a David W. Young and Associates, Inc. and company funded general low level flight research program, a program activated between JANAIR contracts. This brief study of the cutoff element array demonstrated large bandwidths and sufficient coupling to the transmission line, together with very convenient mechanical and construction properties to suggest the cutoff element techniques might be applicable to the JANAIR Rotor Blade Antenna Research Program. This hole technique led to the eventual success of the 173.3 inch leading edge Rotor Blade Antenna. The element technique is equally applicable to the trailing edge. The array is attached very close to the extreme trailing edge of the rotor blade.

The enclosed radar pictures and patterns reflect the feasibility of the leading edge Rotor Blade Antenna. A method of obtaining vertical obstacle information as well as azimuth is also demonstrated.

What was done is emphasized rather than why, and an attempt has been made to make many of the illustrations self explanatory. Some of the patterns contain structural details about the antenna used to generate the pattern and sketches of typical sections. The techniques used to provide the radar picture data are also illustrated.

The final form of the basic array (48-inch length) is sketched in Figure 7, along with a 30 db measured sidelobe pattern which demonstrates performance. This same type array, in the final form was inserted in a 15-inch rotor blade with the proper combination of erosion materials to achieve practical erosion resistance, satisfactory front-to-back ratio, and sufficiently small transmission losses. This final array form in the leading edge of a rotor blade is sketched in Figure 10, complete

with erosion boot and elevation pattern (front-to-back ratio included). Figure 16 and Figure 17 demonstrate the feasibility of the full length 173.3 inch array with far field radiation patterns. Figure 19 is a pattern of the same full length antenna, but focused at 300 feet to a width of 1.57 feet (0.3° beamwidth). Figure 20 relates the beamwidth in feet as a function of range for measured and theoretical arrays focused in the near field and in the far field. Figures 21 through 27 explain the techniques used to provide radar pictures and this same group of figures demonstrates through actual radar picture data the high azimuth resolution capability of the Helicopter Rotor Blade Antenna and also demonstrates a method for obtaining high elevation resolution.

The array was permanently installed in a used UH-1B rotor blade using techniques required to fly the blade. The combination Estane and Neoprene boot was attached to the array-blade assembly, and the final assembly tested. The details of the permanent installation are outlined in Section VIII. Photographs of the installation are included.

Appendix I gives a detailed description of the modification of the commercial oscilloscope for radar PPI measurements and preparation of STC and other timing circuits. STC was not used with the pictures shown in the main body of the report, but perhaps it will be used in the flight test phase. The Crossed Beam Radar technique with its very small elevation beamwidth did not greatly need the STC. However, had STC been used on the PPI, the elevation resolution would have been even further enhanced.

II. SUMMARY

The cutoff element array technique is applicable to both the leading and trailing edges of the rotor blade, indeed it appears the exact same antenna configuration may be used in both the leading and trailing edges. Short antennas were tested in both the leading and trailing edges of the blade with excellent results, but only the leading edge antenna was made full length (173.3 inch aperture). The full length antenna can be tested out of the blade or in the blade for there is little or no difference in the azimuth pattern in either case. The sidelobes and beamwidth change with application of the erosion boot to the leading edge of the blade containing the antenna is negligible. There is a loss of gain of about 1.5 db with .055 inch thick Estane and less loss with thinner pieces. The radiating elements, being at cutoff and certainly not resonant, are affected very little by changes in the element environment caused by the application of erosion material (leading edge), fiberglass cap (trailing edge), and proximity of metal (array in or array out of blade).

The leaky wave mode of radiation was used throughout and although the 30 degree end-fire from broadside beam reduces the effective aperture from 173.3 inches to 150 inches, the experienced phase stability was quite satisfactory. The phase is essentially independent of hole spacing in the final 173 inch antenna. However, large changes in hole spacing in the narrow wall of the waveguide will cause a phase error. This error can be compensated by adjusting the "a" dimension of the waveguide. However, holes in the broadside of the guide, and not too near the edge of the guide, do not cause appreciable phase error. Very large cutoff holes in the narrow side of the guide make the guide appreciably larger, providing a lower than normal cutoff frequency for the guide. The cutoff element technique seems to be particularly applicable to long arrays because of the small required coupling between the radiating element and the waveguide transmission line (about 17 to 40 db).

The thin wall of the waveguide keeps the loss due to the cutoff characteristic of the hole element radiator to about 1 db or less. A nominal wall thickness of .010 inch provides satisfactory results. Control of the wall thickness and of the .030 inch by 173 inch opening above the holes is fairly critical, and poor adjustment and improper handling can raise sidelobe levels from 30 db to 25 db. The proper design sidelobe level suggested 40 db sidelobes, but construction tolerances provided about 30 db sidelobes. It is suspected that flight tests under full load conditions will exhibit sidelobes of anywhere from 25 db to 30 db sidelobes. A 5 db change in sidelobe level at the low level of 30 db can in general antenna practice occur quite easily. The elevation beamwidth of the Rotor Blade Antenna

is about 38 degrees which makes measurement of low sidelobe levels difficult. It is possible the coming flight tests may provide better results than the static field tests because of the obstruction free test site provided by a helicopter at altitude. However, little difference is expected between static field and flying antenna performance data.

The Taylor power distribution employed with the 173.3 inch antenna (150 inch effective) was to provide a theoretical beamwidth of 0.346 degrees, assuming the antenna straight (not bent) and the beamwidth measured at one mile or more. The measured beamwidth at one mile with the antenna bent slightly more than expected under a full load of 121 knots was 0.367 degrees. The measured beamwidth was assumed to be 6 per cent broader because of drag plane deflection. The measured antenna gain was approximately 25 db. The same antenna focused at 300 feet exhibited a measured beamwidth of .3 degrees, a slightly smaller beamwidth than expected. The focused antenna beamwidth at 300 foot range was 1.57 feet wide (.3 degrees), less than the distance between the shoulders of an average man. The antenna has been operated over a wide frequency range with little change in pattern structure, but most of the enclosed patterns were operated at the frequency of 16.2 Kmc since the magnetron available at this facility for radar tests operates at that frequency. Two sets of patterns from 46.6" arrays ranging in frequency from 15 to 50 Kmc demonstrate the broadband capability of the array.

The thin sector slices (20 degrees x 1 degree x several miles) of the radar were displayed similarly to a common PPI (with a conventional PPI radar the elevation beamwidth is much broader) and adequately demonstrated the high azimuth resolution of the rotor blade and the capability of high elevation resolution through the Crossed Beam Technique (References 2 and 3).

While the commerical oscilloscope was oftentimes the limiting factor rather than the antenna, the oscilloscope provided an adequate experimental radar display presentation.

III. ARRAY TECHNIQUE

Early in the program it was found that the leading edge of the rotor blade could be, from a rotor blade structural design aspect, an excellent location for the long array antenna. The main advantage of the leading edge was: if the antenna elevation (or vertical) cross section was small enough, and if the openings in the antenna were not too large, a standard production flyable rotor blade could be modified to accept the antenna and still be airworthy. A flyable trailing edge Rotor Blade Antenna would necessarily require fabrication of a special blade to accept the array. Possible disadvantages of the leading edge were the erosion problem, front-to-back ratio (the microwave energy tends to readily diffract over the leading edge airfoil surface toward the trailing edge) and the requirement for an even smaller elevation cross section array radiator.

The narrow side of the K_q waveguide has neither the proper field current conditions for many slot configurations nor enough vertical height for inclined shunt slots, since the operating frequency is the K_u band. However, it was found that small holes cut in the small side of the waveguide provided sufficient coupling from the guide to free space if the wall thickness were sufficiently thin, and as expected the coupling was very insensitive to frequency change if the hole diameters were well below cutoff for the dominate mode and operating frequency. (Please refer to Section II, Summary). However, it was found that change in hole size apparently affected the cutoff characteristic of the waveguide (changed the wavelength in the guide) and therefore changed both the emerging phase front and thus the beam angle. The broad dimension of the waveguide ("a") could have been slightly decreased to prevent this phase error but it was decided to move the holes to the broad side of the guide. Here too it was found that the holes introduced phase error, but as the holes were moved closer to the longitudinal centerline of the waveguide, the coupling reduced slightly, but the phaseerror rapidly reduced to a negligible value. The holes can be used in the narrow side, there is no doubt, but most of the remaining work reported here is with the holes in the broad side. When a portion of the broad wall is cut away to provide a thin wall for the holes, this same cut away volume can be used as a secondary radiating aperture area, finally leading to a very small cross section radiator. It was found that the coupling to the opening above the holes was quite sensitive to variations in the dimensions of the opening. A thin .010 inch brass plate now covers the holes and good conductivity is assured (soldered) at the joint of the plate and the waveguide. The plate provided the required structural integrity and the electrical conductivity at the junction of the waveguide with the plate. With the plate added, the antenna performed equally well both in and out of the rotor blade. With electrical stability the array

assembly could be epoxied into the rotor blade without critical mechanical features or critical conductivity. Installation of the array is not critical and requires only good aerodynamic practice. The K_a waveguide with its .040 inch wall thickness and 0.25 inch x 0.5 inch outside dimension is the fundamental structure of all arrays demonstrated and reported in this report.

Figure 1 demonstrates the broadband capability of the cutoff element array using the leaky wave mode. The sine of the angle of the main beam with respect to broadside is proportional to the ratio of the free space wavelength to the wavelength in the guide. Change in frequency causes a corresponding change in beam angle, but unlike resonant slots with critical slot spacing, the pattern shape generated by the cutoff element, leaky wave array, is largely independent of frequency.

The antenna is more broadband without the use of the opening in the brass nose section of the rotor blade, probably due to the frequency sensitivity of the short at the junction of the brass leading edge with the waveguide back of the hole elements. However, Figure 2 adequately demonstrates the broadband capability of the array in the brass leading edge. Figure 3 is a plot of the normalized relative gain of a horn whose gain varies with the square of the free space wavelength and the gain of the array, which is assumed to vary only as a function of wavelength. Theoretical and measured gains are shown.

When the data for Figure 4 were taken it was not intended to indicate effective dimensional change in the waveguide broad dimension (a) with hole position, and the data taken may not be accurate enough, but it is certain that holes in the narrow side do increase the "a" dimension effectively by lowering the cutoff frequency or decreasing the wavelength in the guide. The extreme hole diameters used in the 173.3 inch array were found to exhibit little phase error. Why the curve which demonstrates radiation from holes in the broadside (near the center line) is not coincident with the theoretical curve, is not quite certain. However, the lower ends of the curve are within the specified tolerance of the waveguide as given by the original manufacturer.

While the bandwidth of the array in the brass leading edge is less than in free space (no brass plate), the bandwidth of the array in either condition is greater than the HP-628A signal generator bandwidth which was used for these pattern measurements. The only limit to bandwidth of the basic array is probably the transmission line and perhaps a ridged line would give greater bandwidth. An octave bandwidth does seem a possibility (2/1 frequency change).

Figures 1 and 2 used symmetrical power coupling about the center of the array, while using a high per cent of power in the load to achieve a near symmetrical power taper. Figures 5 and 6 used the same array with constant coupling (holes to the transmission line) and a high per cent of power in the load to achieve a nearly uniform power distribution. These patterns were all used to confirm phase linearity prior to building the long array.

Figure 7 is representative of the final basic array configuration of short length (46.4 inches). Note particularly the sketch of the array which is different than the preceding figures. The final basic array form shown in Figure 7 contains the brass plate as an integral part of the basic array and the .030 inch slit is the secondary radiator.

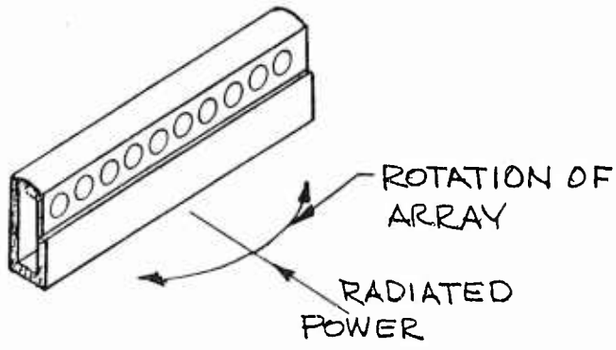

SECTION OF 50" ARRAY

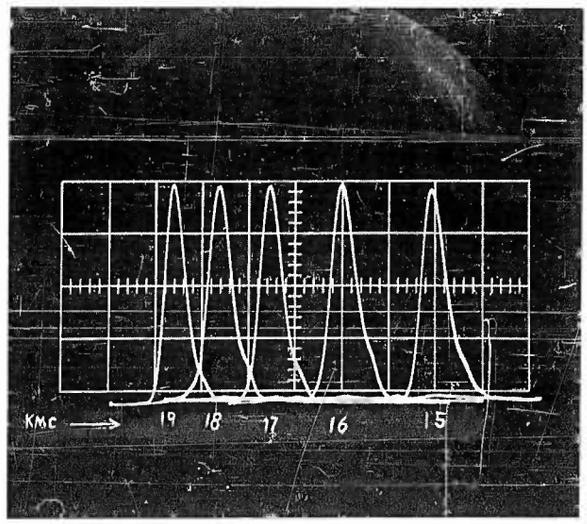

FREQUENCY: 15.0 TO 19.0 KMC
RANGE: 37.5 FEET (INDOOR)
APERTURE: 46.6 INCHES
FREQUENCY SCAN: 21.15°
DATA SCALE: HORIZONTAL; 3.8°/CM
VERTICAL; 1 V/CM

50" ARRAY PATTERN
LARGE BANDWIDTH DEMONSTRATION

FIGURE 1

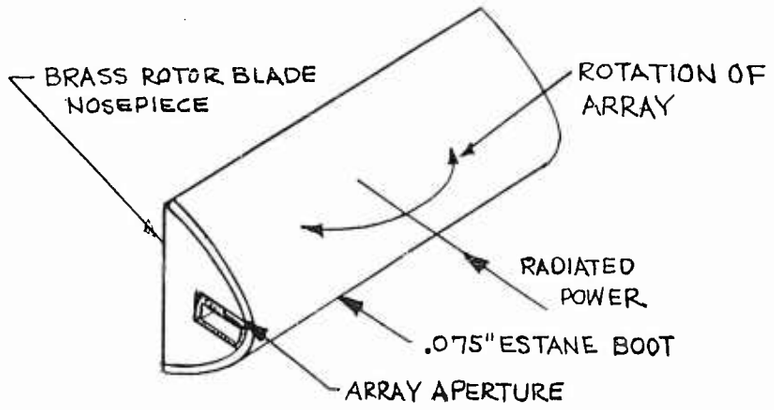

SECTION OF 50" ARRAY

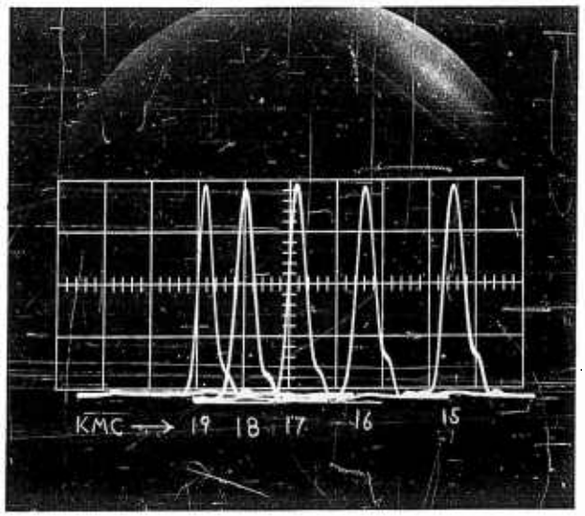

FREQUENCY : 15.0 TO 19.0 KMC
RANGE : 37.5 FEET (INDOOR)
APERTURE : 46.6 INCHES
DATA SCALE : HORIZONTAL ; 3.8°/CM
VERTICAL ; 1 V/CM

FREQUENCY (KMC)	PRINCIPAL LOBE (DEGREES, ENDFIRE FROM BROADSIDE)
15	23.0
16	29.5
17	36.0
18	40.0
19	44.0

50" ARRAY PATTERN
LARGE BANDWIDTH DEMONSTRATION

FIGURE 2

Predicted relative gain is an inverse function of λ: Horn gain is an inverse function of λ^2, and the Array gain is an inverse function of λ.

Antenna Measured: 50", 343 hole, cutoff element array, high per cent of power in load. Minimum hole spacing .094", maximum 210". Maximum hole diameter .094", minimum .063".

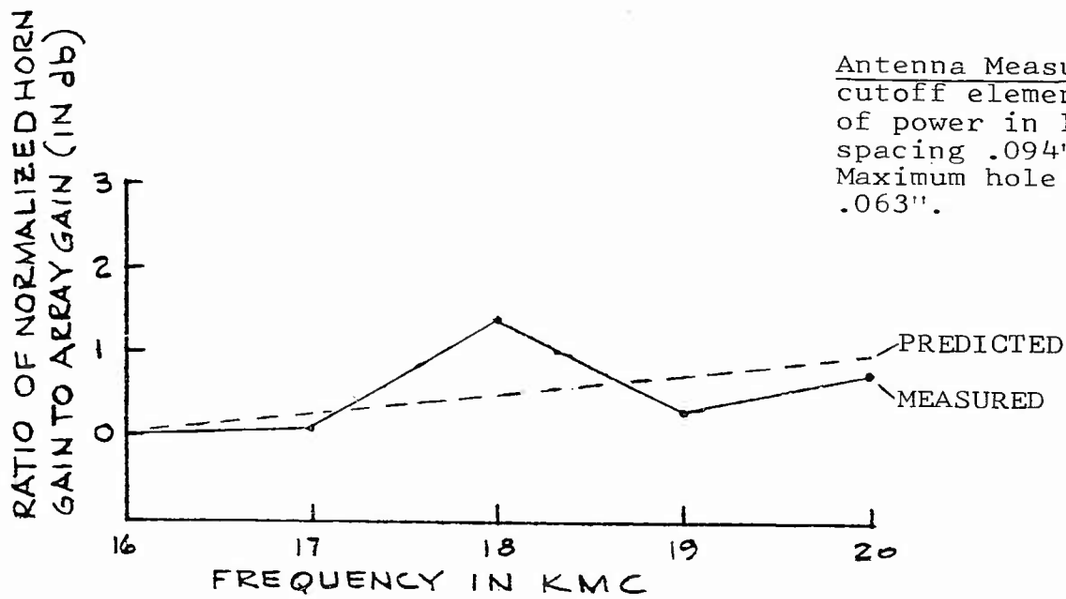

DEMONSTRATION OF BROAD BAND ARRAY: The coupling of the radiating elements to the transmission line is essentially independent of frequency. The change in effective element spacing with large changes in frequency has little effect on the pattern, since the element spacing is very small with respect to a wavelength.

FIGURE 3

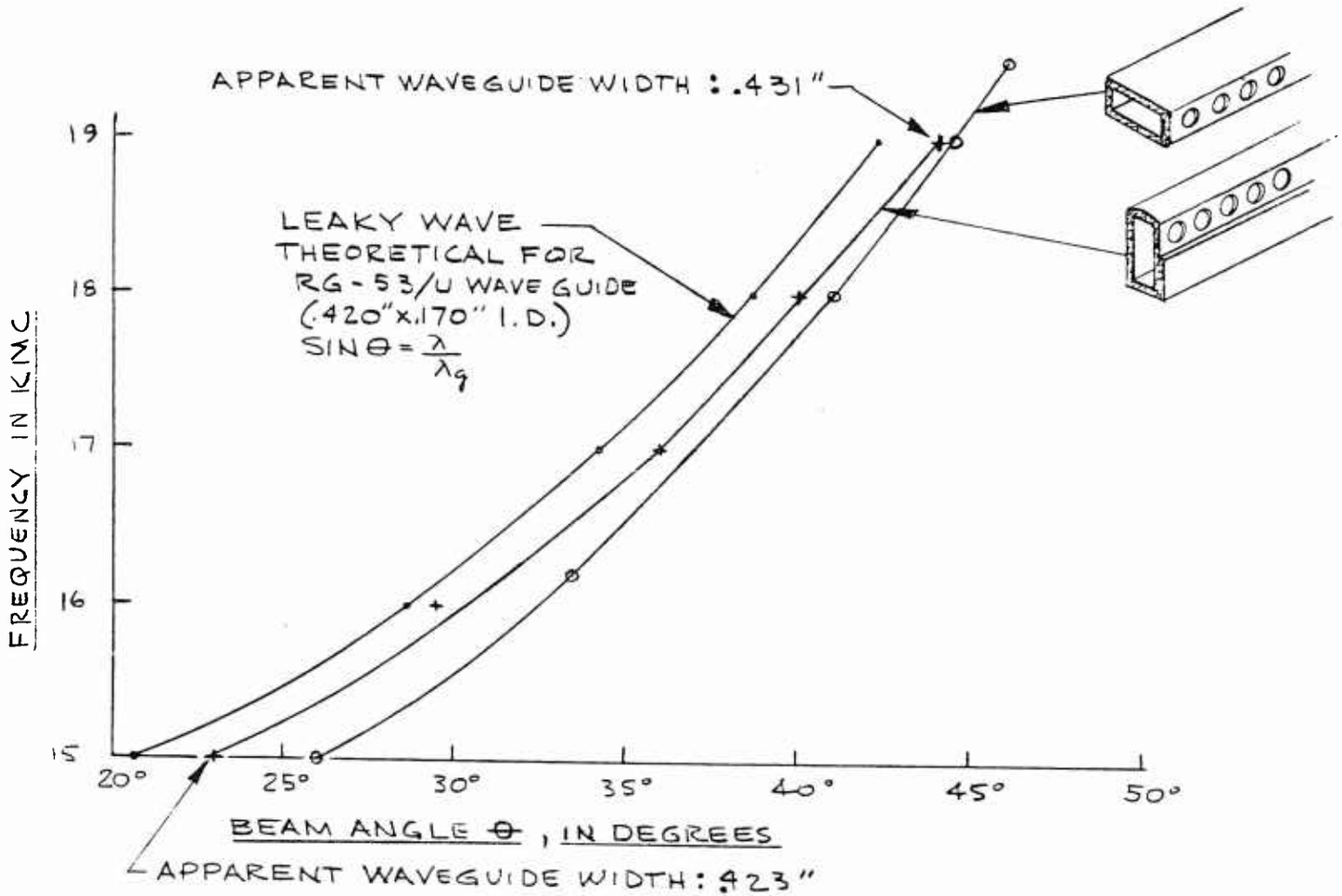

BEAM ANGLE, IN DEGREES ENDFIRE FROM BROADSIDE

FIGURE 4

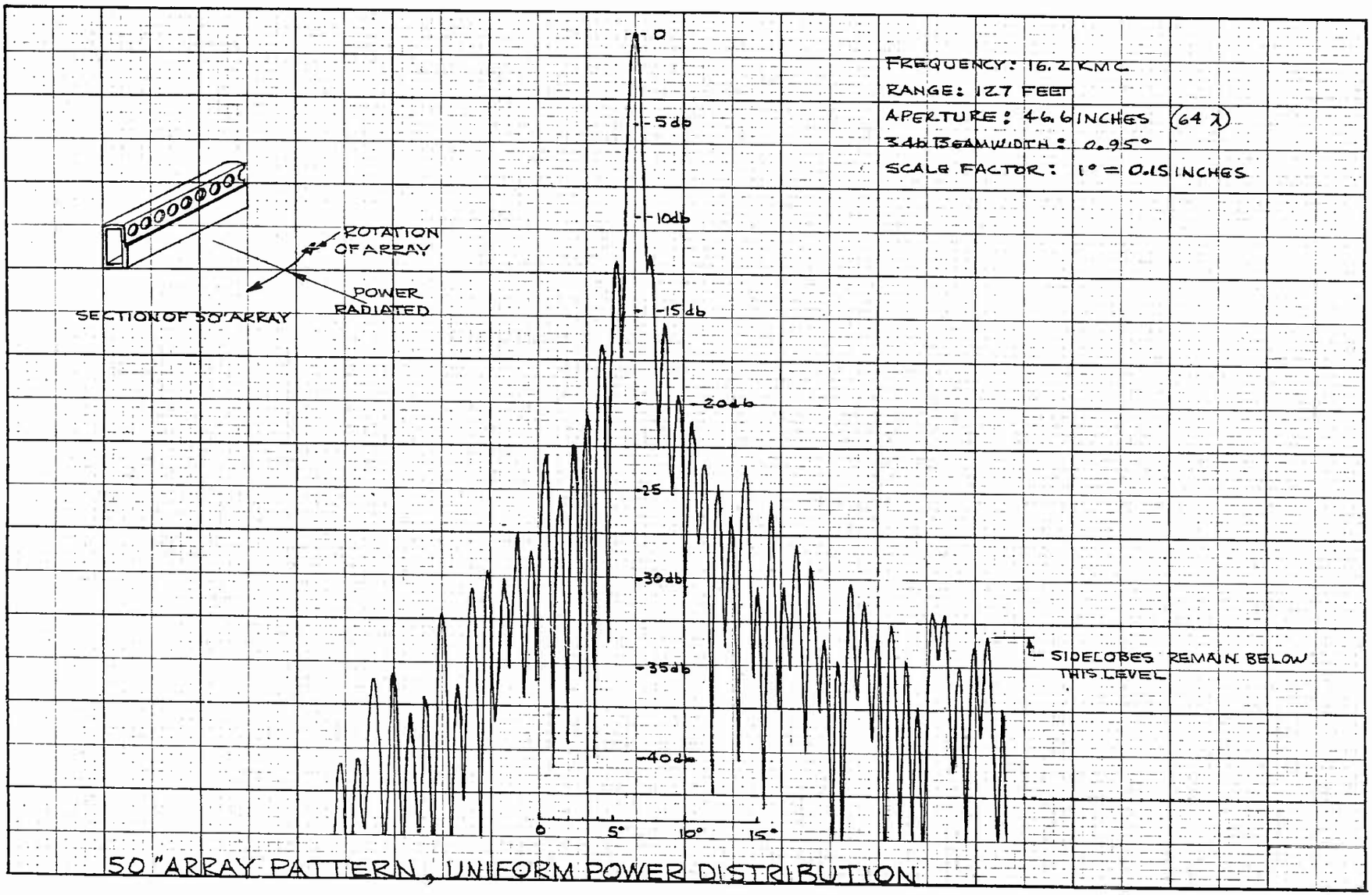
FREQUENCY: 16.2 KMC
RANGE: 127 FEET
APERTURE: 46.6 INCHES (64 λ)
3db BEAMWIDTH: 0.95°
SCALE FACTOR: 1° = 0.15 INCHES
-0
-5db
-10db
-15db
-20db
-25
-30db
-35db
-40db
0
5°
10°
15°
ROTATION OF ARRAY
POWER RADIATED
SECTION OF 50' ARRAY
SIDELOBES REMAIN BELOW THIS LEVEL
50" ARRAY PATTERN, UNIFORM POWER DISTRIBUTION

FIGURE 5

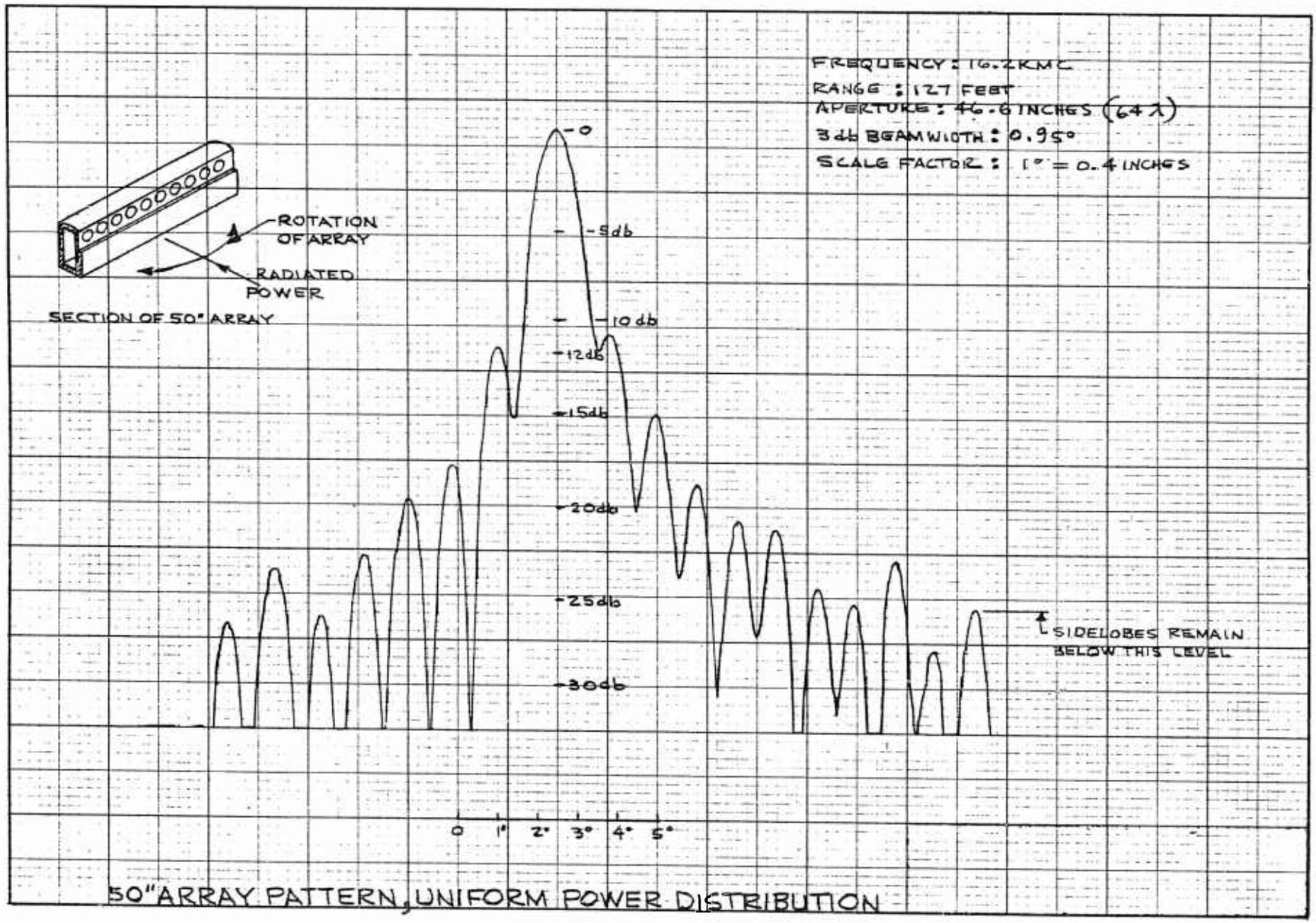
FREQUENCY: 16.2KMC
RANGE: 127 FEET
APERTURE: 46.6 INCHES (64λ)
3db BEAMWIDTH: 0.95°
SCALE FACTOR: 1° = 0.4 INCHES
ROTATION OF ARRAY
RADIATED POWER
SECTION OF 50" ARRAY
-0
-5db
-10db
-12db
-15db
-20db
-25db
-30db
SIDELOBES REMAIN BELOW THIS LEVEL
0 1° 2° 3° 4° 5°
50" ARRAY PATTERN, UNIFORM POWER DISTRIBUTION

FIGURE 6

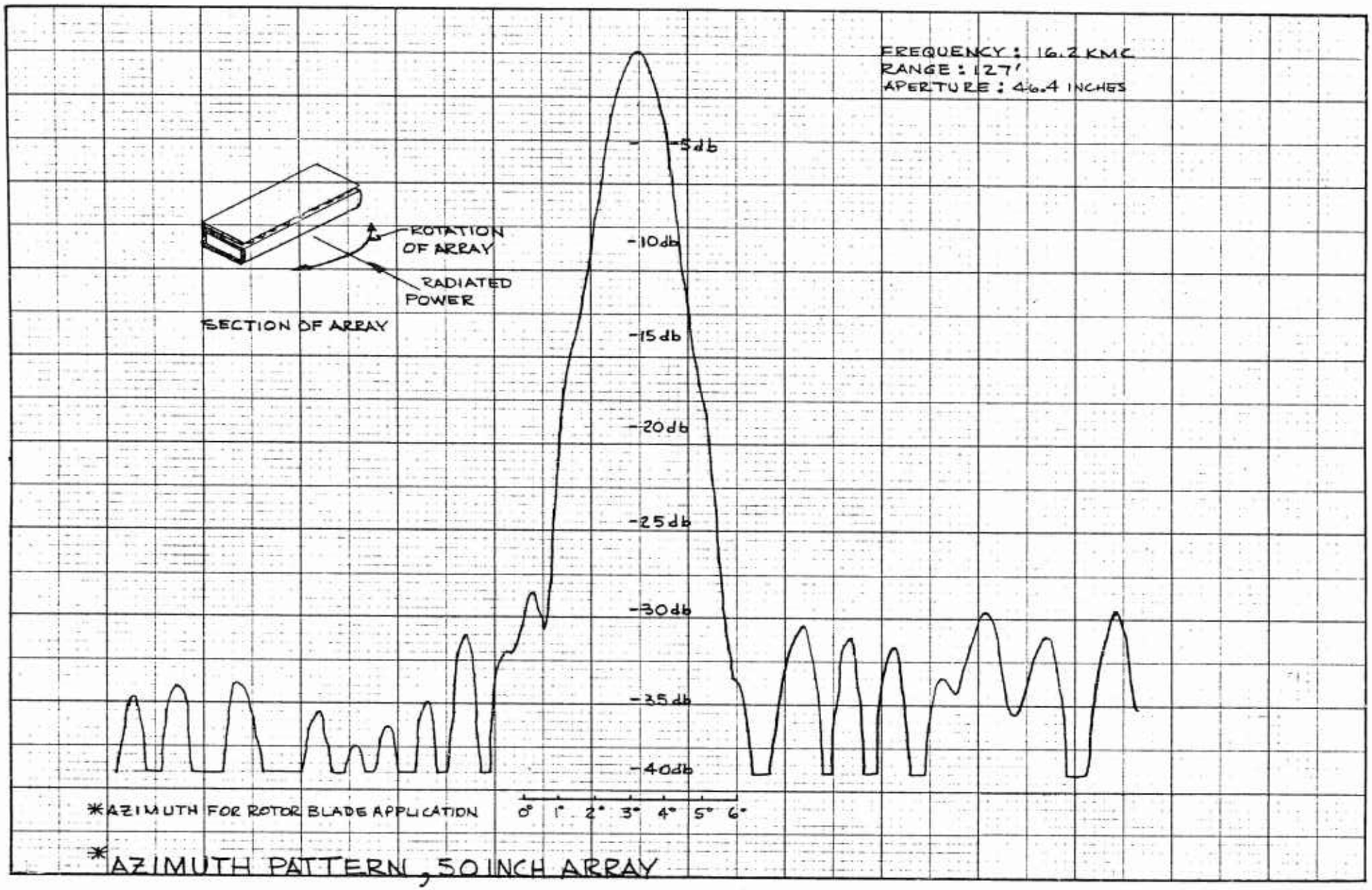
FREQUENCY : 16.2 KMC
RANGE : 127'
APERTURE : 46.4 INCHES
-5db
-10db
-15db
-20db
-25db
-30db
-35db
-40db
ROTATION OF ARRAY
RADIATED POWER
SECTION OF ARRAY
*AZIMUTH FOR ROTOR BLADE APPLICATION
0° 1° 2° 3° 4° 5° 6°
*AZIMUTH PATTERN, 50 INCH ARRAY

FIGURE 7

IV. FRONT TO BACK RATIO

Fifteen inch rotor blade sections were cut to aid in detailed measurements of the element radiator environments and some of these same sections were used for elevation pattern measurements, but it was soon realized that new sections cut on a 30 degree bias had to be prepared to make meaningful front to back ratio measurements with convenient short sections. Figures 8 and 9 are typical of the square cut sections. The array shown has holes in the broad side and is not typical but the slot in the leading edge of the rotor blade section and the trailing edge configuration is typical. The remaining small blade sections were cut on a 30 degree bias because the beam angle is 30 degrees from the broad side. This angle is typical of the leaky wave mode with a wavelength in the guide twice the length of the free space wavelength. Both the forward main lobe and a diffraction lobe to the rear are 30 degrees from the broad side beams.

Figure 10 is the elevation pattern of both the forward and reverse lobe with the complete final assembly, including the proper combination of Estane and Neoprene to provide both erosion and suppression of the back lobe. While the back lobe suppression (front to back ratio) has not been optimized, 20 db is believed satisfactory. Twenty-five db should not be very difficult to achieve, but 30 db will be quite a bit more difficult. The back lobe is a surface wave and has rather small elevation beamwidth, having an effective aperture of about seven inches. Perhaps this feature could be put to good use but for the present program the surface wave effect serves no useful purpose.

Figure 11 is the elevation pattern of a leading edge antenna without Neoprene. Thus, the back beam is not absorbed. This back lobe causes no difficulty if the rotor blade is used to transmit and a vertical antenna is used for receiving (Crossed Beam Technique). Since the vertical antenna will have a broad azimuth pattern but probably no more than 180 degrees, the receiving antenna may be switched off when the back lobe from the helicopter blade passes into the visible frontal view. However, when the rotor blade is used for both transmit and receive, the back lobe is no different than any other side lobe and may cause a serious display error by printing each obstacle twice, one correctly and one displayed 120 degrees (a considerable error). However, the 20 db sidelobe level provided by the microwave absorbent Neoprene is quite sufficient for most performance requirements.

The trailing edge antenna (Figure 12) performs quite well and has much less tendency to produce a lobe toward the leading edge (naturally good front to back ratio). A small, very thin conductive sheet is required to balance the back radiation

toward the leading edge to minimize the back lobe. Again, the back lobe suppression has not been optimized, but the 20 db is believed to be satisfactory. Good front to back ratio seems somewhat easier to provide with the trailing edge antenna. There is very little transmission difficulty with the fiberglas airfoil fairing.

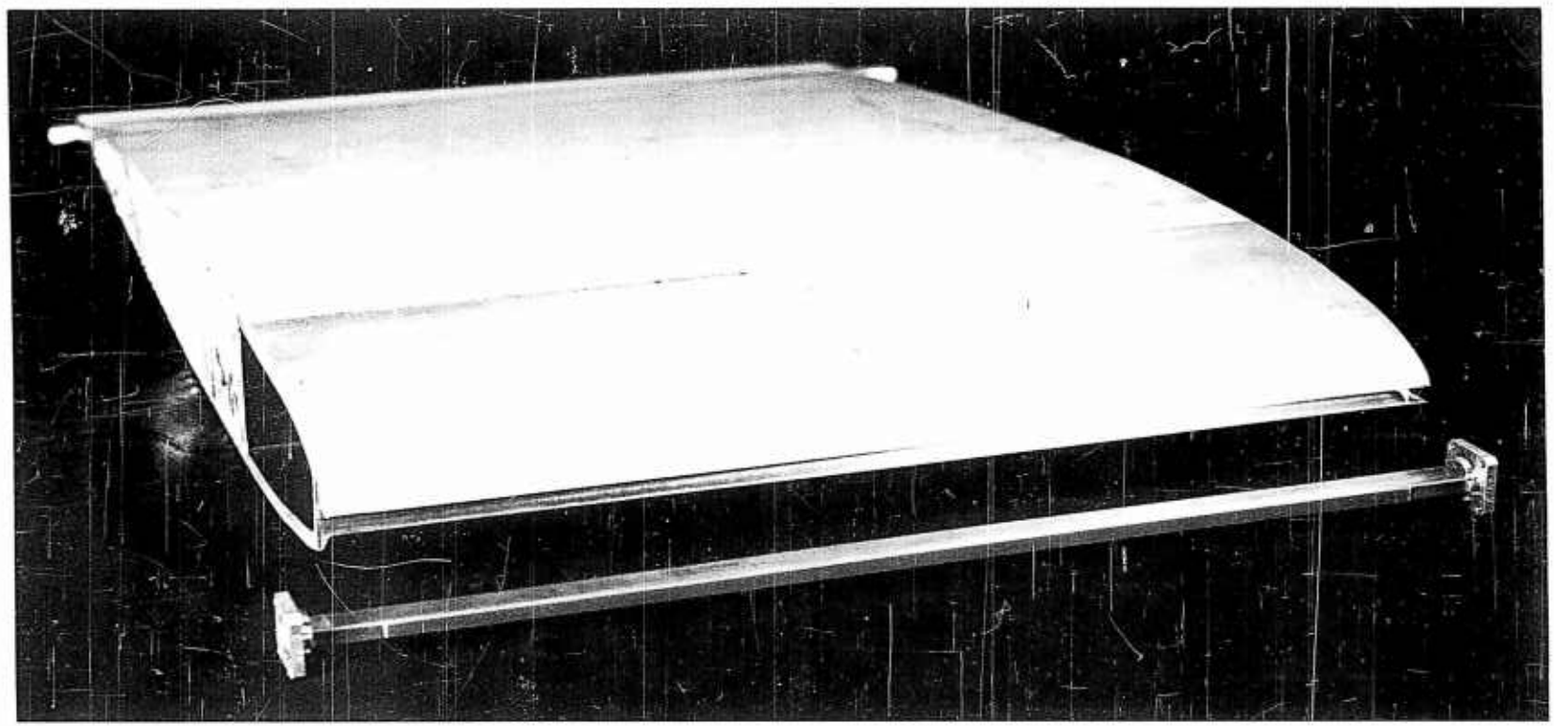

15-INCH ROTOR SECTION FOR ARRAY ELEMENT
ENVIRONMENT MEASUREMENT AND ELEVATION PATTERNS

FIGURE 8

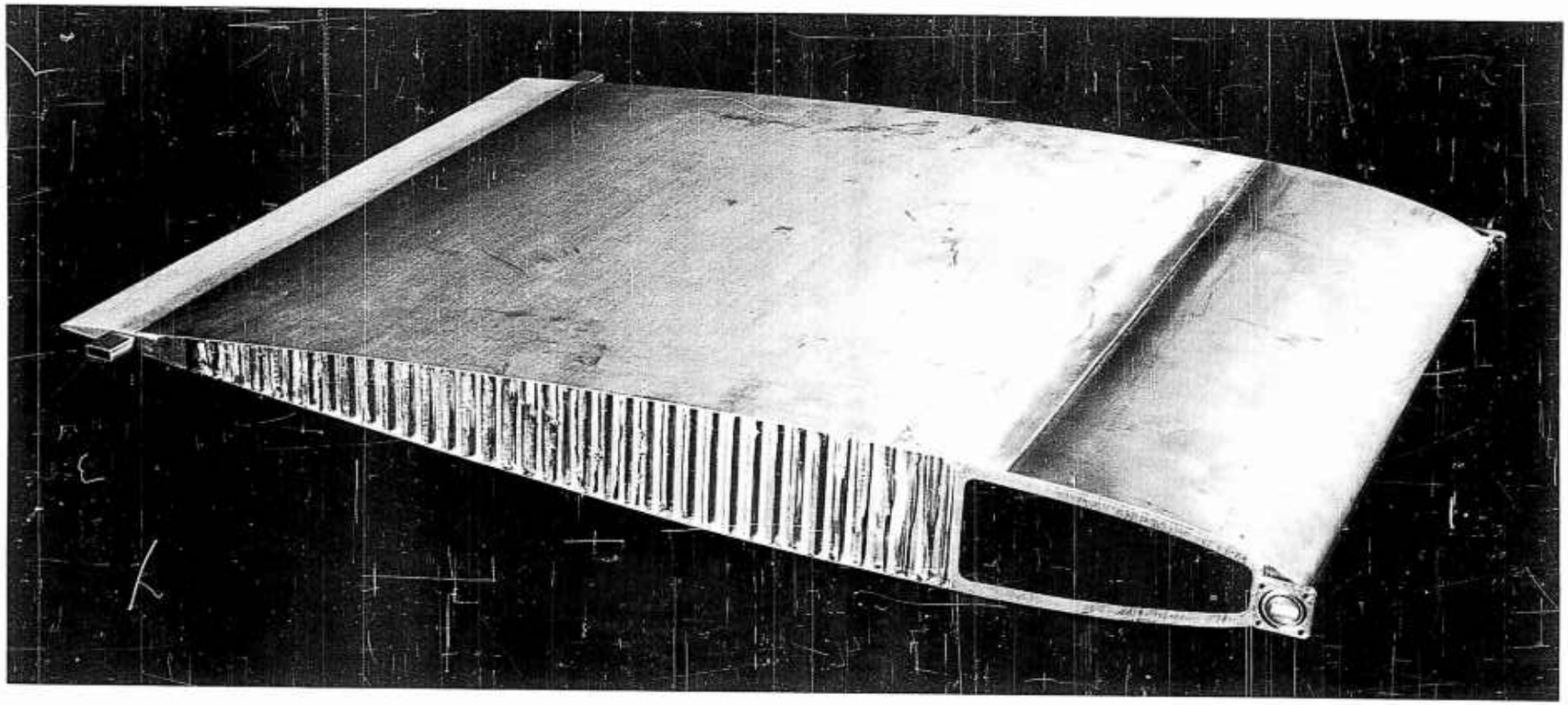

15-INCH ROTOR SECTION FOR ARRAY ELEMENT
ENVIRONMENT MEASUREMENT AND ELEVATION PATTERNS

FIGURE 9

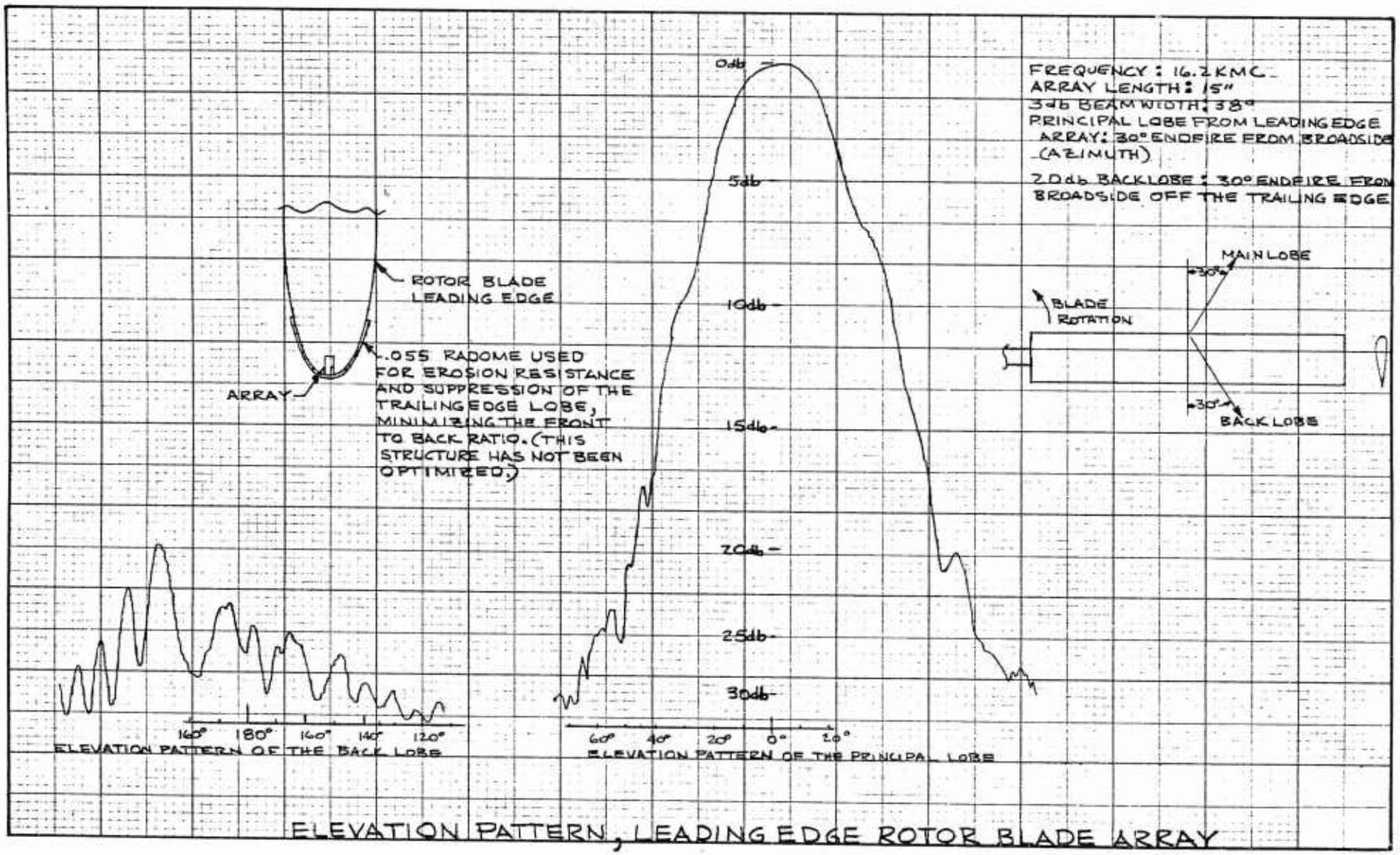
FREQUENCY: 16.2 KMC
ARRAY LENGTH: 15"
3db BEAM WIDTH: 38°
PRINCIPAL LOBE FROM LEADING EDGE ARRAY: 30° ENDFIRE FROM BROADSIDE (AZIMUTH)
20db BACKLOBE: 30° ENDFIRE FROM BROADSIDE OFF THE TRAILING EDGE
ROTOR BLADE LEADING EDGE
ARRAY
.055 RADOME USED FOR EROSION RESISTANCE AND SUPPRESSION OF THE TRAILING EDGE LOBE, MINIMIZING THE FRONT TO BACK RATIO. (THIS STRUCTURE HAS NOT BEEN OPTIMIZED)
0db
5db
10db
15db
20db
25db
30db
MAIN LOBE
BLADE ROTATION
BACK LOBE
160° 180° 160° 140° 120°
ELEVATION PATTERN OF THE BACK LOBE
60° 40° 20° 0° 20°
ELEVATION PATTERN OF THE PRINCIPAL LOBE
ELEVATION PATTERN, LEADING EDGE ROTOR BLADE ARRAY

FIGURE 10

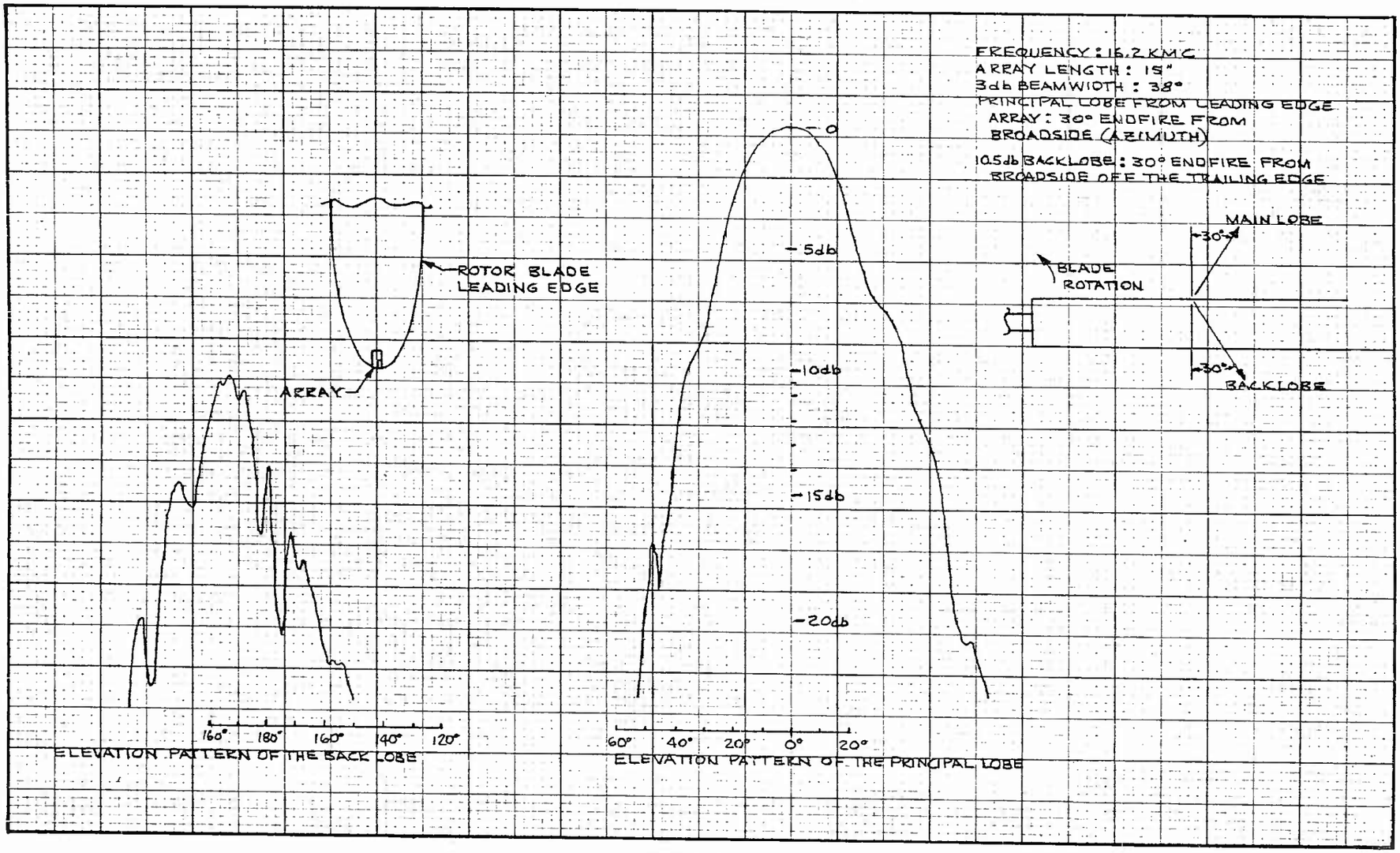
FREQUENCY: 16.2 KMC
ARRAY LENGTH: 15"
3db BEAMWIDTH: 38°
PRINCIPAL LOBE FROM LEADING EDGE ARRAY: 30° ENDFIRE FROM BROADSIDE (AZIMUTH)
10.5db BACKLOBE: 30° ENDFIRE FROM BROADSIDE OFF THE TRAILING EDGE
MAIN LOBE
30°
BLADE ROTATION
30°
BACKLOBE
ROTOR BLADE LEADING EDGE
ARRAY
0
-5db
-10db
-15db
-20db
160° 180° 160° 140° 120°
ELEVATION PATTERN OF THE BACK LOBE
60° 40° 20° 0° 20°
ELEVATION PATTERN OF THE PRINCIPAL LOBE

FIGURE 11

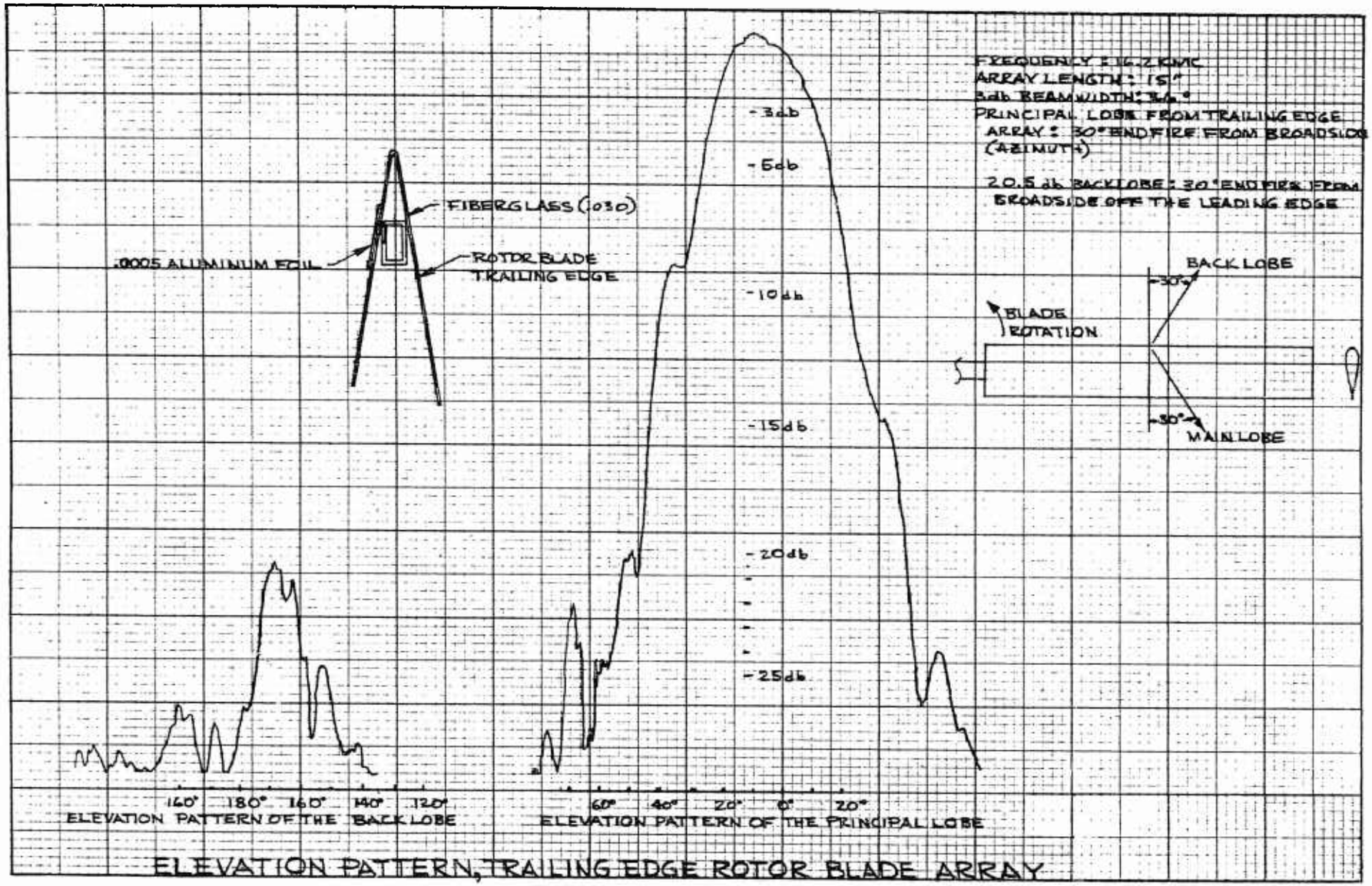

ELEVATION PATTERN, TRAILING EDGE ROTOR BLADE ARRAY

FIGURE 12

V. 173.3 INCH ARRAY DESIGN

Figure 13 is a plot of the hole coupling as a function of the position on the array. The method of calculating coupling, together with the variation in hole sizes used, and the effects of a lossy transmission line are shown. The statement in parenthesis "(a similar technique for half wave or more spacing)" was meant to imply the cutoff hole technique could be used for an array which used element spacing to determine the main beam angle, usually a half wavelength or more. While the curve shown was normalized, the peak value of coupling (the closest coupling) was about 17 db. The transmission line loss reduced the gain of the antenna 1.5 db, a reasonably small figure.

Figure 14 itemizes the equipment used to provide the patterns for the full length Rotor Blade Antenna. The figure further details the instrumentation schematic and the physical layout of equipment. The actual antenna pattern measurement site is shown in Figure 15. Both the Rayleigh range and the far field range is shown.

Figures 16, 17, and 18 are final patterns of the finished array. Figure 16 is most complete and the data detailed on Figure 16 apply equally well to Figure 17 and largely to Figure 18. Figure 16 and Figure 17 differ slightly in sidelobe structure and level and it is not known why, but this small change in sidelobe level can occur because of the broad elevation beamwidth of the array and slight scattering from the ground cover. Most of the difference in Figures 16 and 17 is scale factor, however. The data itemized are self-explanatory.

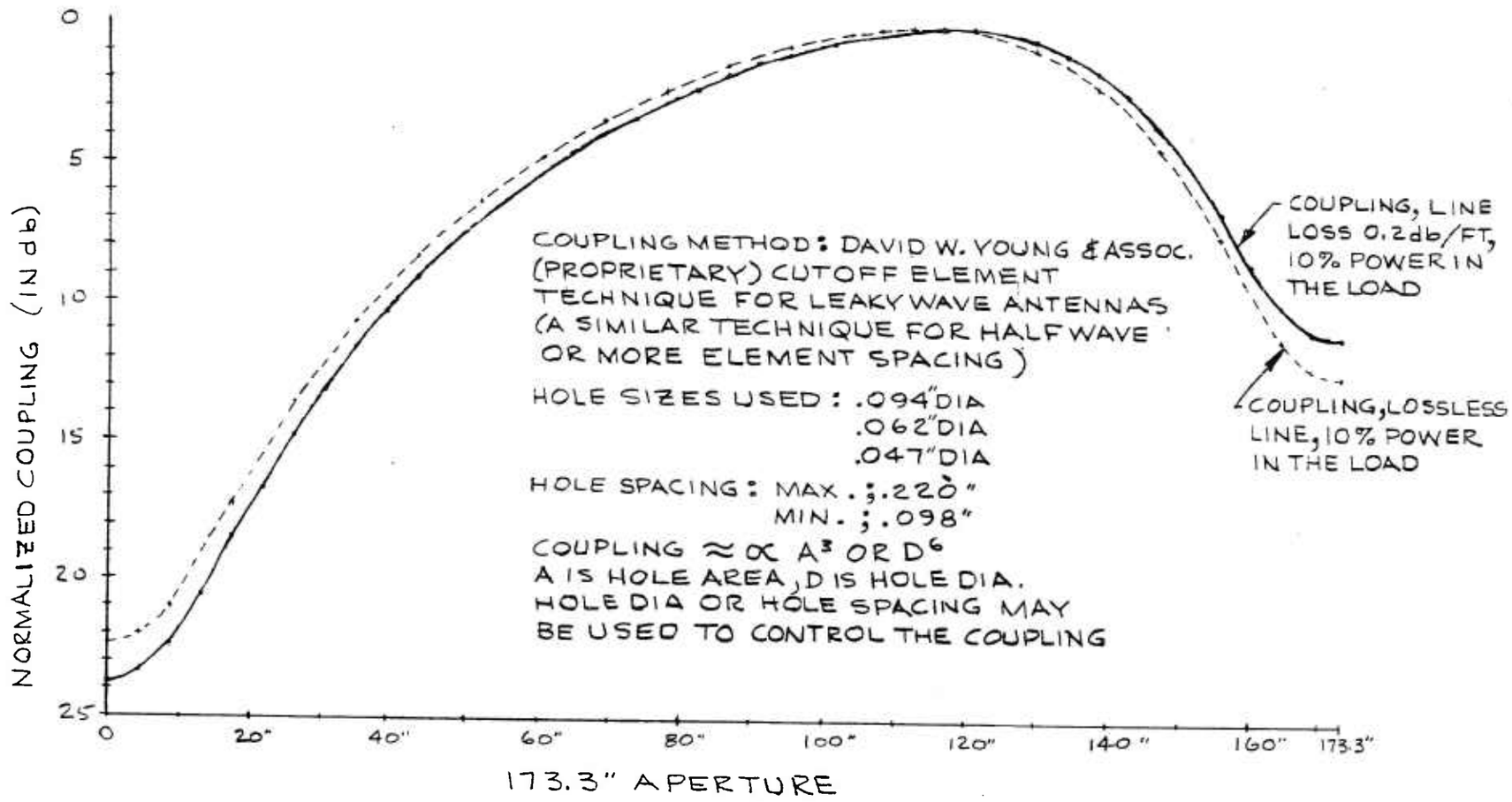

COUPLING CURVE FOR TAYLOR DISTRIBUTION 40db SIDELOBES $\bar{n} = 10$

FIGURE 13

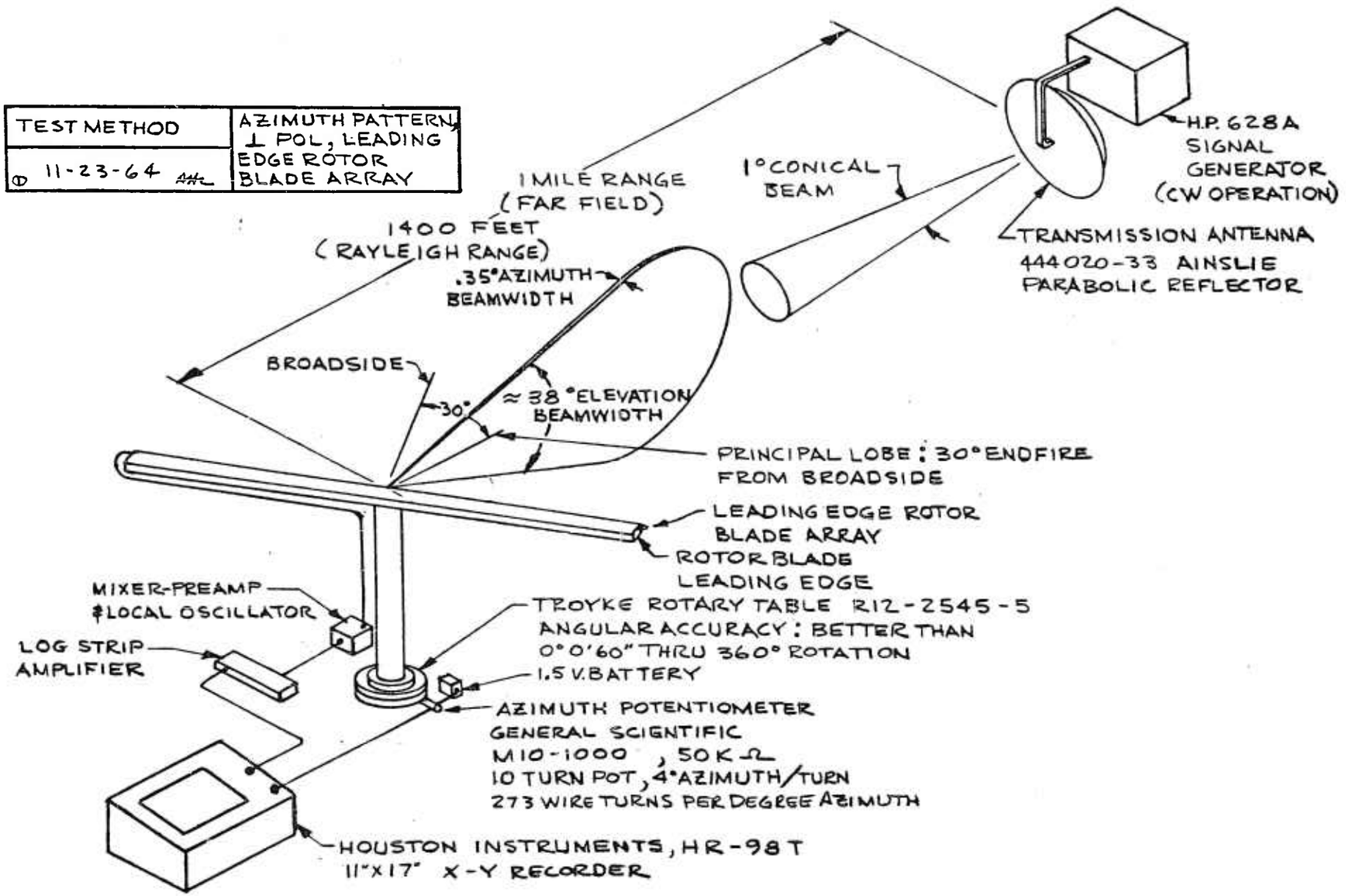
TEST METHOD
AZIMUTH PATTERN, ⊥ POL, LEADING EDGE ROTOR BLADE ARRAY
Φ 11-23-64
1 MILE RANGE (FAR FIELD)
1400 FEET (RAYLEIGH RANGE)
1° CONICAL BEAM
H.P. 628A SIGNAL GENERATOR (CW OPERATION)
TRANSMISSION ANTENNA 444020-33 AINSLIE PARABOLIC REFLECTOR
.35° AZIMUTH BEAMWIDTH
BROADSIDE
30°
≈ 38° ELEVATION BEAMWIDTH
PRINCIPAL LOBE: 30° ENDFIRE FROM BROADSIDE
LEADING EDGE ROTOR BLADE ARRAY
ROTOR BLADE LEADING EDGE
MIXER-PREAMP & LOCAL OSCILLATOR
LOG STRIP AMPLIFIER
TROYKE ROTARY TABLE R12-2545-5
ANGULAR ACCURACY: BETTER THAN 0°0'60" THRU 360° ROTATION
1.5 V. BATTERY
AZIMUTH POTENTIOMETER
GENERAL SCIENTIFIC
M10-1000, 50K Ω
10 TURN POT, 4° AZIMUTH/TURN
273 WIRE TURNS PER DEGREE AZIMUTH
HOUSTON INSTRUMENTS, HR-98T
11"X17" X-Y RECORDER

FIGURE 14

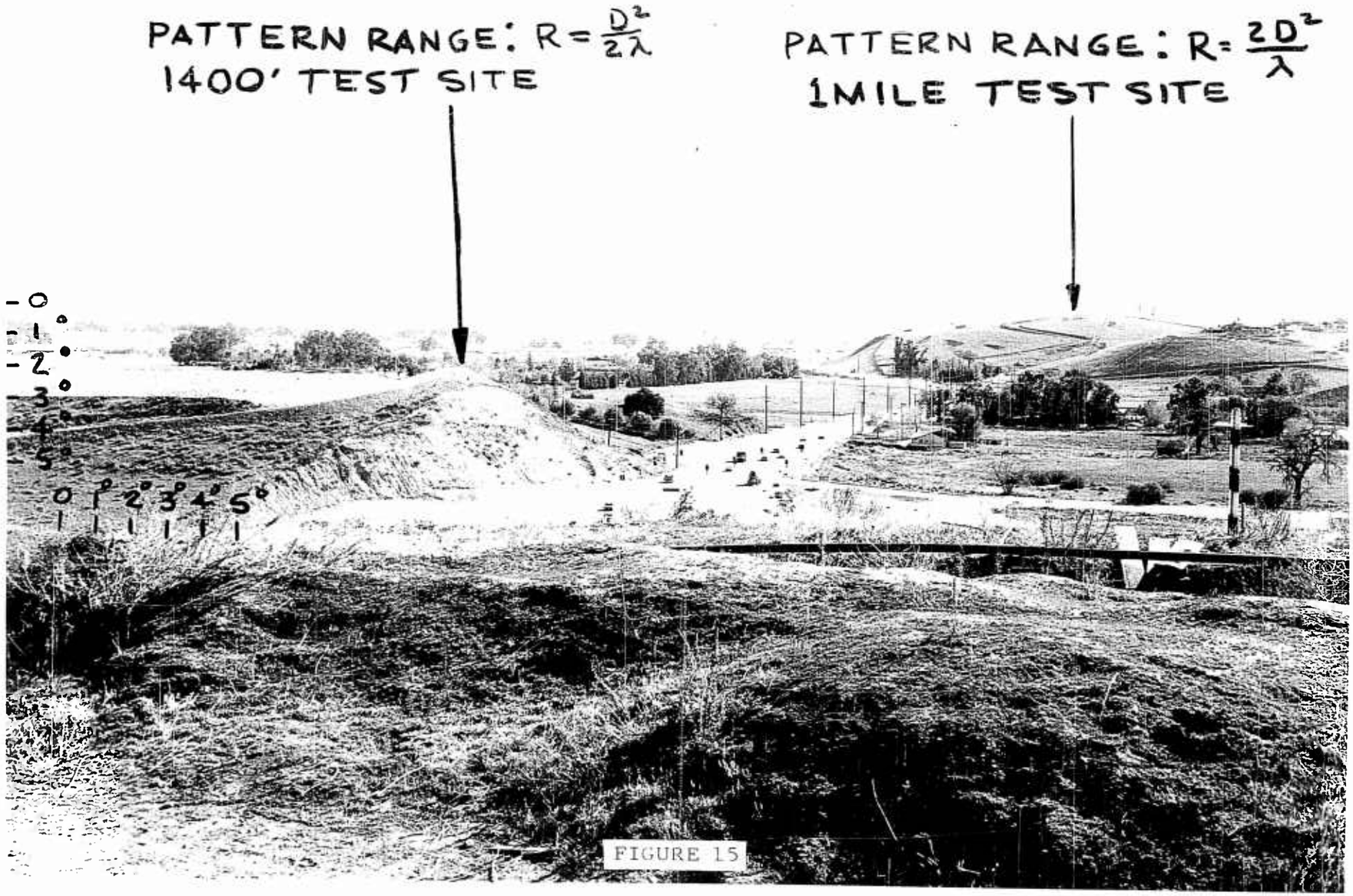
PATTERN RANGE: $R = \frac{D^2}{2\lambda}$
1400' TEST SITE
PATTERN RANGE: $R = \frac{2D^2}{\lambda}$
1 MILE TEST SITE
0°
-1°
-2°
-3°
-4°
-5°
0° 1° 2° 3° 4° 5°

FIGURE 15

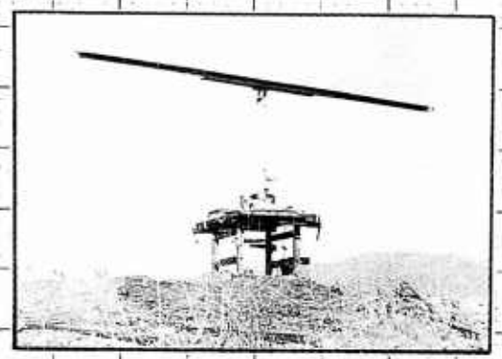

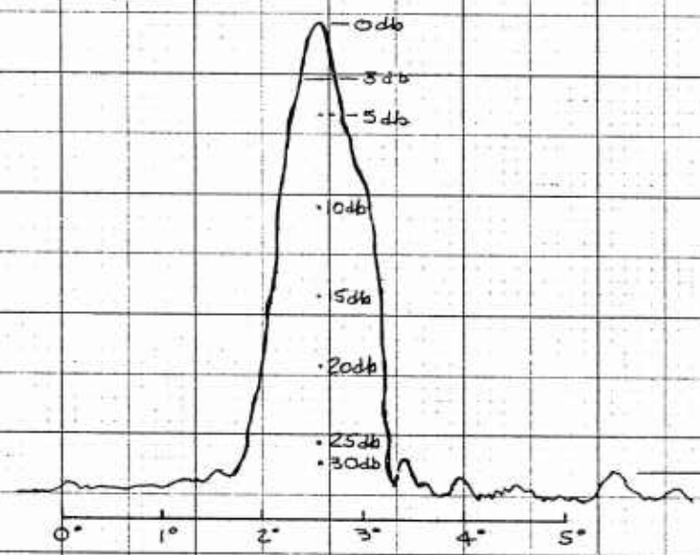

FREQUENCY: 16.2 KMC
173.3 APERTURE ARRAY #1
RANGE 1 MILE

PRINCIPLE LOBE: 30° ENDFIRE FROM BROADSIDE

3 db BEAMWIDTH: .367° (MEASURED)

BEAMWIDTH FOR TAYLOR DISTRIBUTION (40db SIDELOBES, $\bar{n}$ = 10) WITH ADJUSTED APERTURE OF 150" (DUE TO 30° FROM BROADSIDE): .346°

THIS INDICATES 6% BEAMBROADENING WITH .19" DRAG PLANE BENDING & .25" DROOP OVER THE 15' ANTENNA LENGTH

NOTE: THE .19" EXCEEDS THE MAXIMUM DEFLECTION OF BLADE DURING 120 KNOT FLIGHT LOAD CONDITION AT THE MAXIMUM BLADE DEFLECTION ANGLE (PSI REF. #11)

MEASURED GAIN ≅ 25 dB (NO ESTANE) AND CONTAINS 1.5db LOSS IN THE K_a WAVEGUIDE

THEORETICAL GAIN 26db

AZIMUTH PATTERN, LEADING EDGE ROTOR BLADE ARRAY

FIGURE 16

DETAILS: SEE PRECEDING PATTERN (FIG. 16)

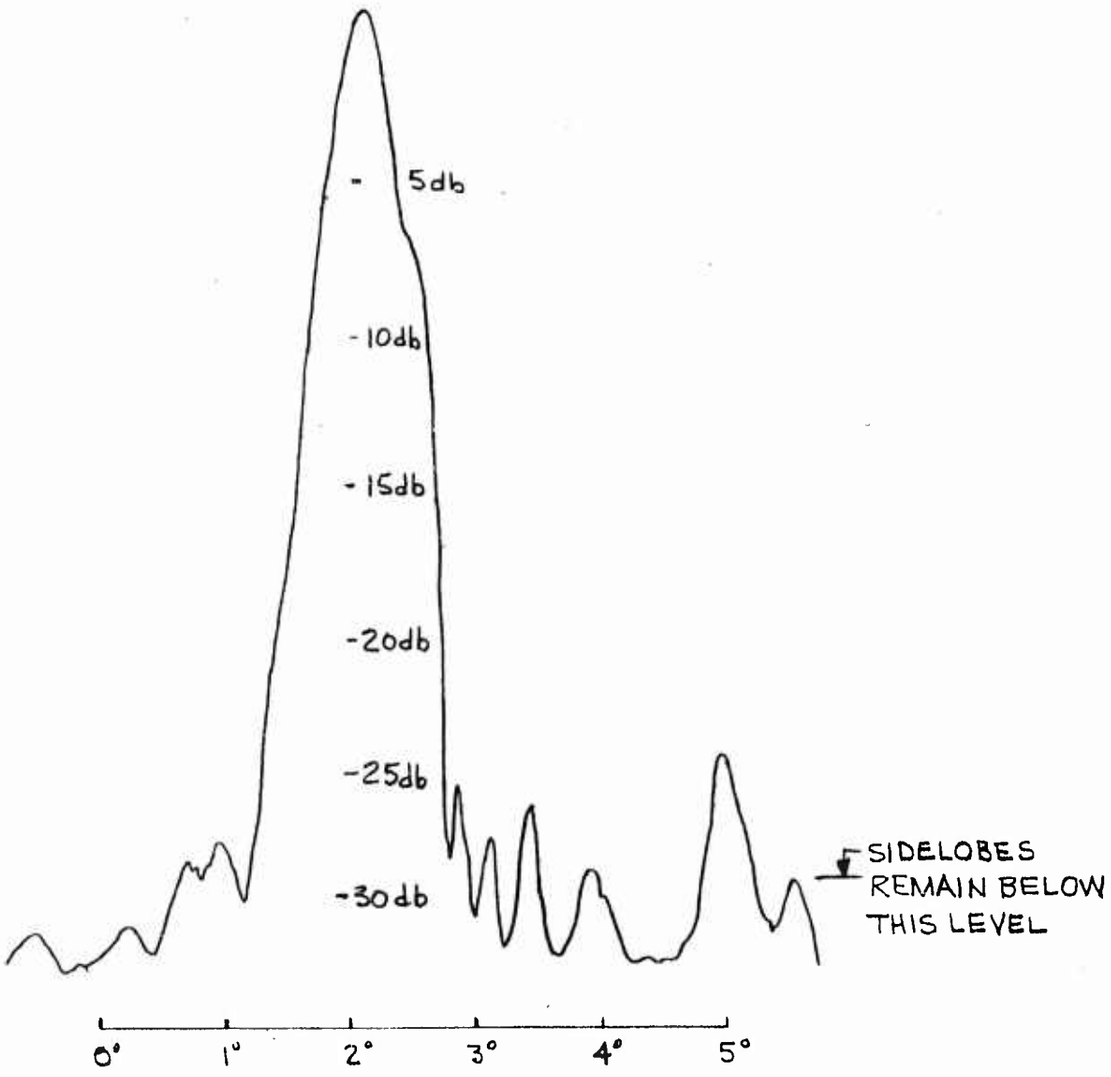

AZIMUTH PATTERN, LEADING EDGE ROTOR BLADE ARRAY

FIGURE 17

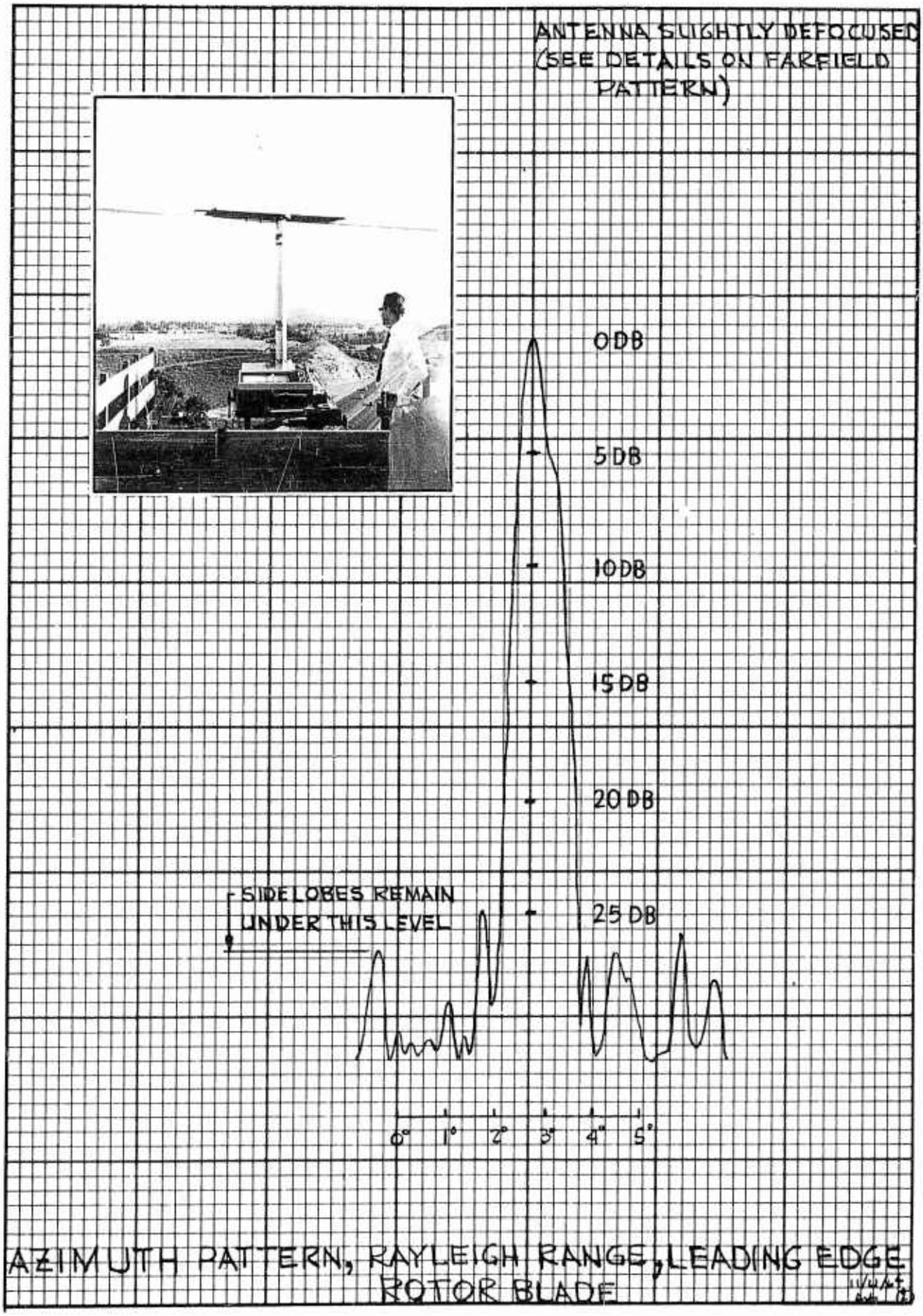
ANTENNA SLIGHTLY DEFOCUSED
(SEE DETAILS ON FARFIELD
PATTERN)
0DB
5DB
10DB
15DB
20DB
25DB
SIDELOBES REMAIN
UNDER THIS LEVEL
0°
1°
2°
3°
4°
5°
AZIMUTH PATTERN, RAYLEIGH RANGE, LEADING EDGE
ROTOR BLADE

FIGURE 18

VI. EFFECTS OF FOCUSING

There are only two figures with this section, Figure 19 and Figure 20. At first glance the figures are deceptively simple and seem of little significance, but the relationship between an antenna focused in the near field and the far field and the relationship between the resolution of an array in the near field, when focused at infinity, or slightly defocused, is seldom understood. The following measurements may make these resolution relations at 3 db clearer for this particular 173.3 inch antenna.

Figure 19 is the pattern of the 173.3 inch array focused at 300 feet and exhibits low sidelobes and a beamwidth of 1.57 feet, corresponding to 0.3 degrees.

Figure 20 illustrates the following: the beamwidth of the array measured in feet is the same at the aperture for all conditions of phase including focus at near and far field and defocused. The beamwidth at the aperture is simply the power distribution of the array, in this case the Taylor distribution for 40 db sidelobes, $\bar{n} = 10$. If the antenna had a uniform power distribution instead of the symmetrical power taper, the beamwidth at the aperture would be about 15 feet instead of 5 feet. The beamwidth of the focused antenna is not a point (or line) as in geometric optics, but is limited to the basic beamwidth of the array. The beamwidth of the array at distances other than the focal distance is shown at the left side of Figure 20. While comparing the measured beamwidth in feet for the array under full load conditions (slightly defocused) at various ranges (it is not a straight line function) it is interesting to remember that beamwidth in the far field is proportional to the ratio of array aperture to wavelength, while the Rayleigh range is proportional to the ratio of the array aperture squared to the wavelength, which might suggest a higher operating frequency for the same resolution with a subsequent reduction in the Rayleigh range. However, the antenna can only be effectively focused for improved resolution in the Rayleigh range. No conclusion has been drawn but these relations are being considered. Many practical uses of the rotor blade will in the future take place in the present Rayleigh range of the 173.3 inch K_u band antenna (the Rayleigh range is approximately 1400 feet).

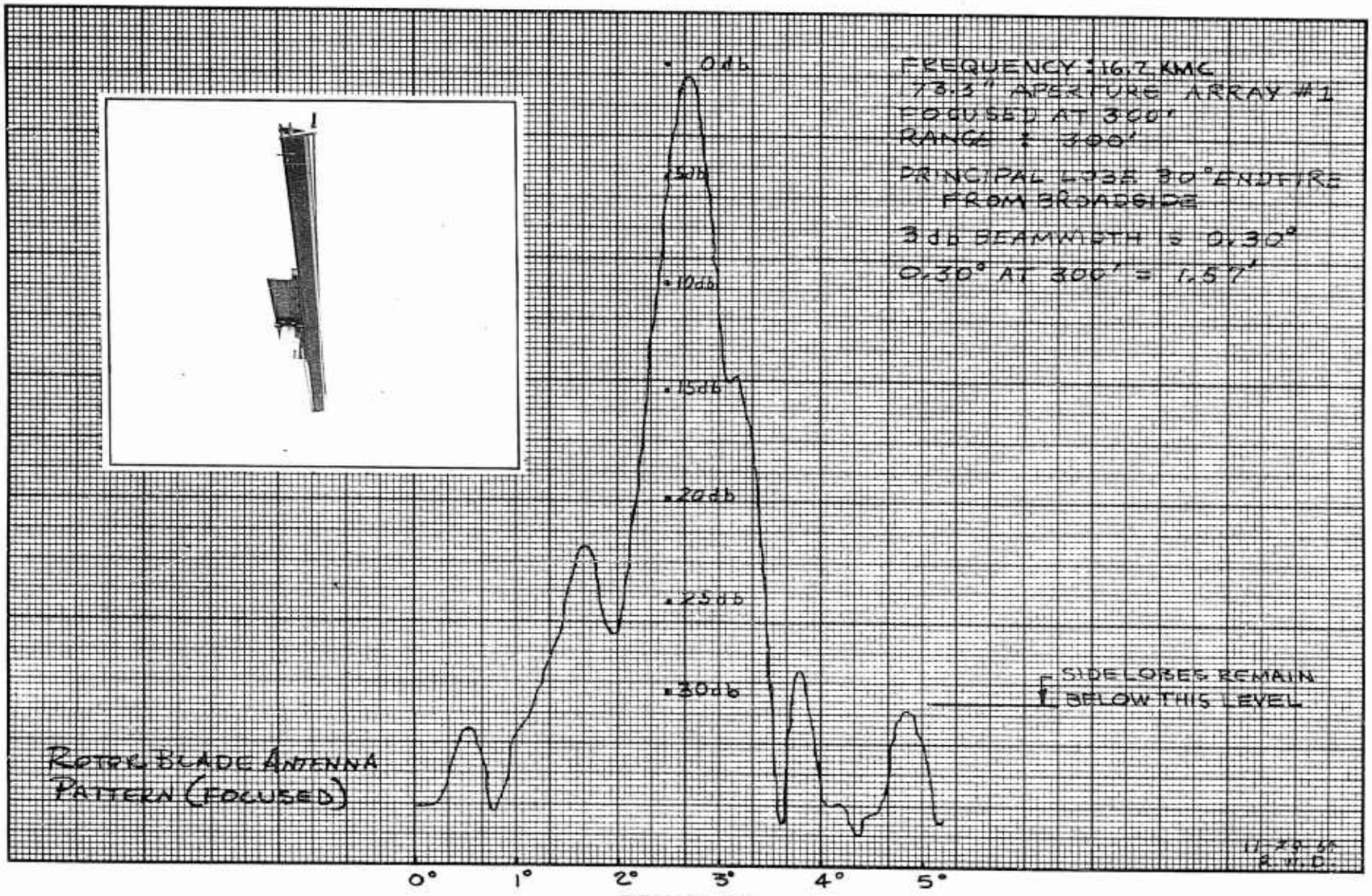
0db
-5db
-10db
-15db
-20db
-25db
-30db
FREQUENCY: 16.7 KMC
73.3" APERTURE ARRAY #1
FOCUSED AT 300'
RANGE = 300'
PRINCIPAL LOBE 30° ENDFIRE FROM BROADSIDE
3 db BEAMWIDTH = 0.30°
0.30° AT 300' = 1.57'
SIDE LOBES REMAIN BELOW THIS LEVEL
ROTEL BLADE ANTENNA PATTERN (FOCUSED)
0°
1°
2°
3°
4°
5°

FIGURE 19

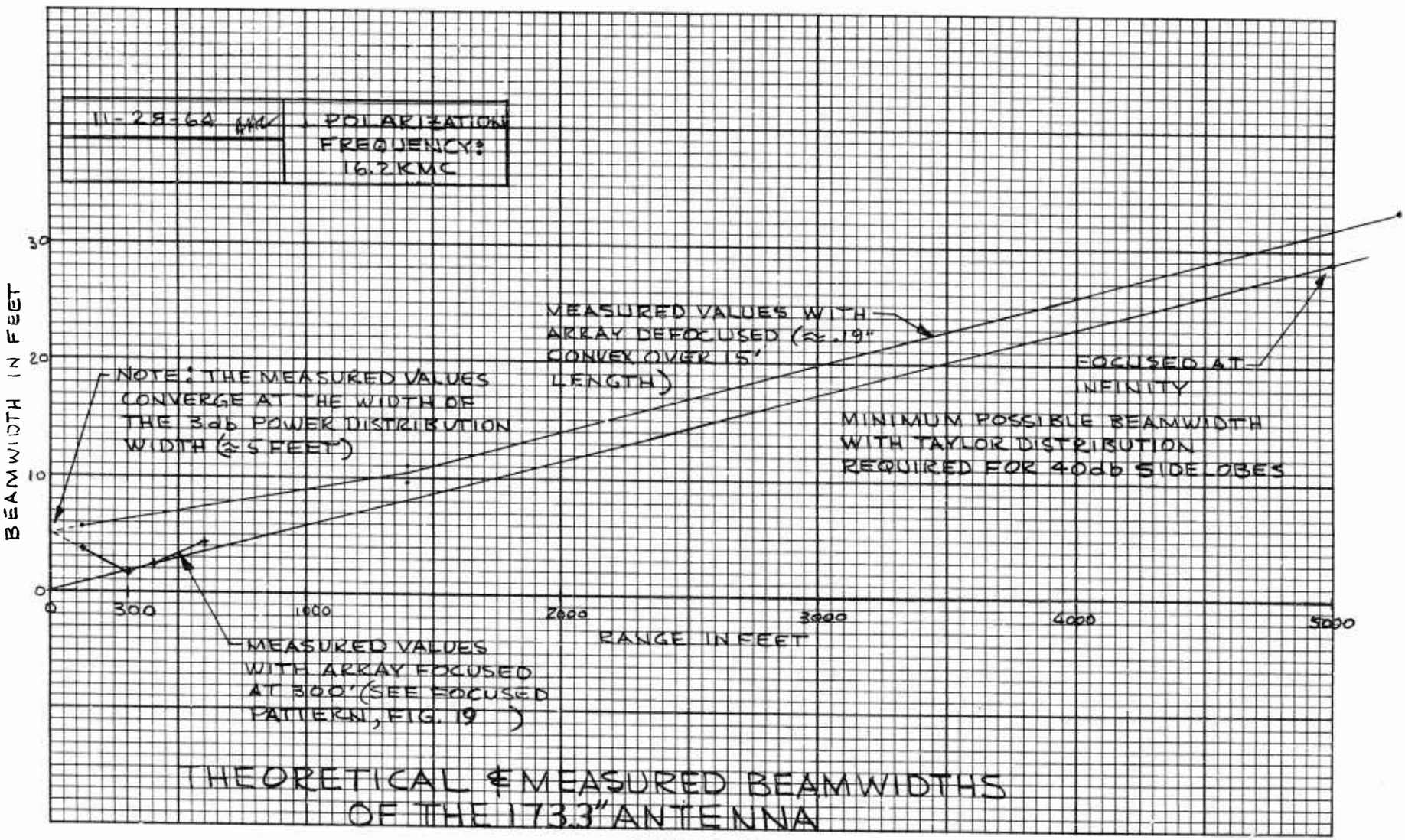
11-28-64
POLARIZATION
FREQUENCY:
16.2 KMC
BEAMWIDTH IN FEET
30
20
10
0
0
300
1000
2000
3000
4000
5000
RANGE IN FEET
NOTE: THE MEASURED VALUES CONVERGE AT THE WIDTH OF THE 3db POWER DISTRIBUTION WIDTH (≈ 5 FEET)
MEASURED VALUES WITH ARRAY DEFOCUSED (≈ .19" CONVEX OVER 15' LENGTH)
FOCUSED AT INFINITY
MINIMUM POSSIBLE BEAMWIDTH WITH TAYLOR DISTRIBUTION REQUIRED FOR 40db SIDE LOBES
MEASURED VALUES WITH ARRAY FOCUSED AT 300' (SEE FOCUSED PATTERN, FIG. 19)
THEORETICAL & MEASURED BEAMWIDTHS OF THE 1733" ANTENNA

FIGURE 20

VII. RADAR AND OPTICAL PHOTOGRAPHIC COMPARISONS

Figure 21 illustrates the equipment layout and electromagnetic technique for obtaining the radar results shown in Figures 23, 25, and 27. Thin PPI sector slices were used having the dimensions of 20 degrees azimuth, one degree elevation and some particular value of range for each slice.

Figure 22 shows the actual antenna configurations employed for the thin slice PPI radar data. Figure 22 also indicates the edgeview orientation of the four PPI radar slices shown in Figure 23 which correspond to the following elevation angles; 0 degrees, 1 degree, 2 degrees, and 5 degrees. The radar sectors are shown in Figure 23. The slide at 5 degrees elevation has a ten mile full scale range and the other slices (0 degrees, 1 degree, 2 degrees) have a full scale range of two miles each. The transmitter power was in all cases about 4,000 watts peak power with a pulse width of about 0.125 us. Aerial photographs for both two miles and ten miles full scale are shown in Figure 23. No STC (receiver sensitivity time control) was employed, but even so, the crispness which "Stony Point" appears and disappears with one degree displacement of the sector slice is excellent. The small amount of "Stony Point" shown in the one degree slice is actually the lower portion of the "Stony Point" which can be seen on larger negatives not included.

The power poles shown at four miles and ten miles, the train, the wooden poles at 0.5 to one mile, small metal poles, corn field, etc. in Figure 25 and 27, point to the feasibility of not only high azimuth resolution but obstacle detection through use of high elevation resolution. Only obstacles were accentuated. Figure 24 provides an optical view of the radar targets or obstacles shown in Figure 25. Figure 26 is an optical view of the obstacles shown in Figure 27. In Figure 26 the very close hill and closer trees are also shown on the radar, Figure 27.

These simple photographs suggest great airborne radar system capability.

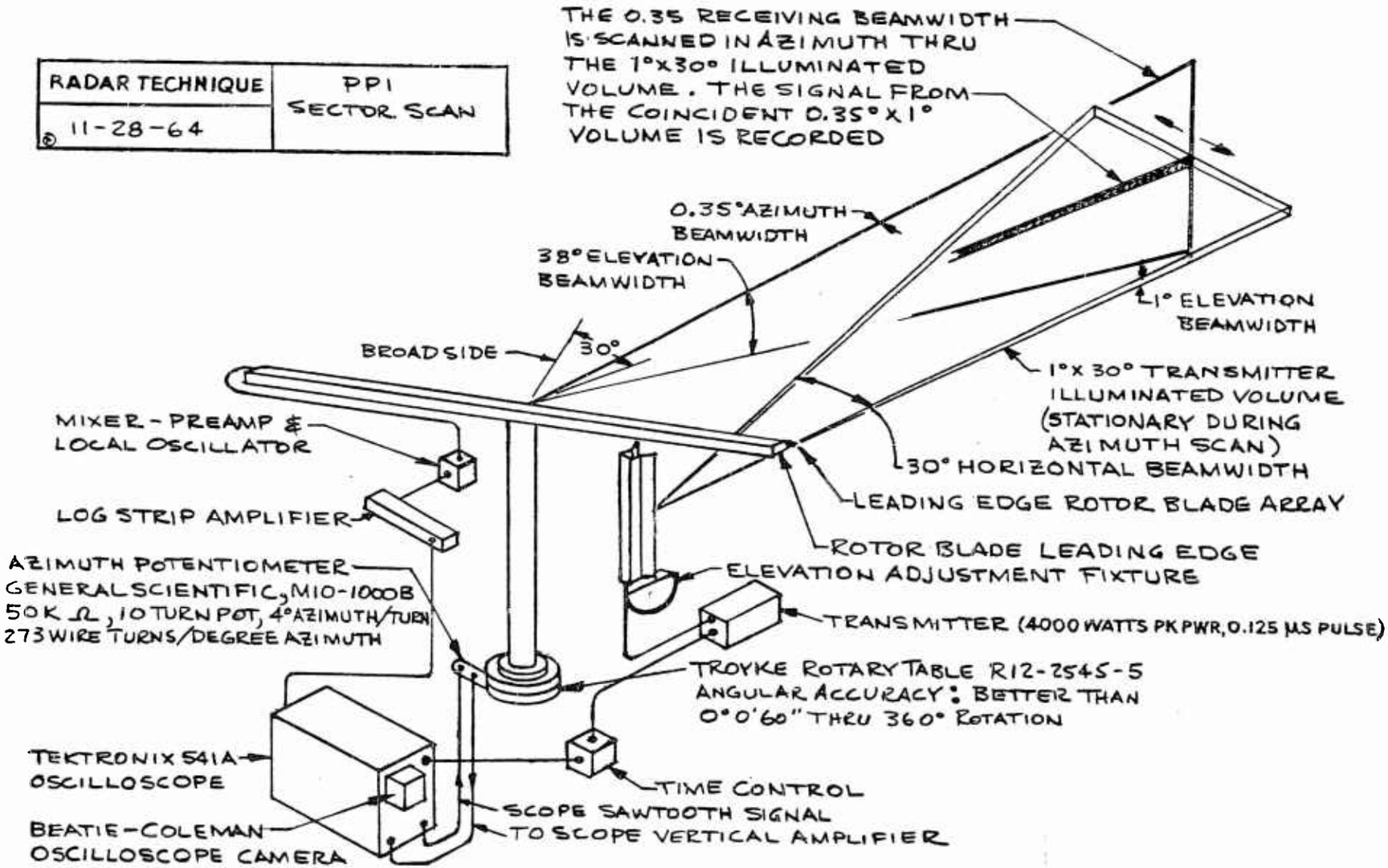
RADAR TECHNIQUE
PPI SECTOR SCAN
11-28-64
THE 0.35 RECEIVING BEAMWIDTH IS SCANNED IN AZIMUTH THRU THE 1°x30° ILLUMINATED VOLUME. THE SIGNAL FROM THE COINCIDENT 0.35°x1° VOLUME IS RECORDED
0.35° AZIMUTH BEAMWIDTH
38° ELEVATION BEAMWIDTH
1° ELEVATION BEAMWIDTH
BROADSIDE
30°
1°x 30° TRANSMITTER ILLUMINATED VOLUME (STATIONARY DURING AZIMUTH SCAN)
30° HORIZONTAL BEAMWIDTH
LEADING EDGE ROTOR BLADE ARRAY
ROTOR BLADE LEADING EDGE
ELEVATION ADJUSTMENT FIXTURE
MIXER - PREAMP & LOCAL OSCILLATOR
LOG STRIP AMPLIFIER
AZIMUTH POTENTIOMETER GENERAL SCIENTIFIC, M10-1000B 50K Ω, 10 TURN POT, 4° AZIMUTH/TURN 273 WIRE TURNS/DEGREE AZIMUTH
TRANSMITTER (4000 WATTS PK PWR, 0.125 μS PULSE)
TROYKE ROTARY TABLE R12-2545-5 ANGULAR ACCURACY: BETTER THAN 0°0'60" THRU 360° ROTATION
TEKTRONIX 541A OSCILLOSCOPE
TIME CONTROL
SCOPE SAWTOOTH SIGNAL TO SCOPE VERTICAL AMPLIFIER
BEATIE-COLEMAN OSCILLOSCOPE CAMERA

FIGURE 21

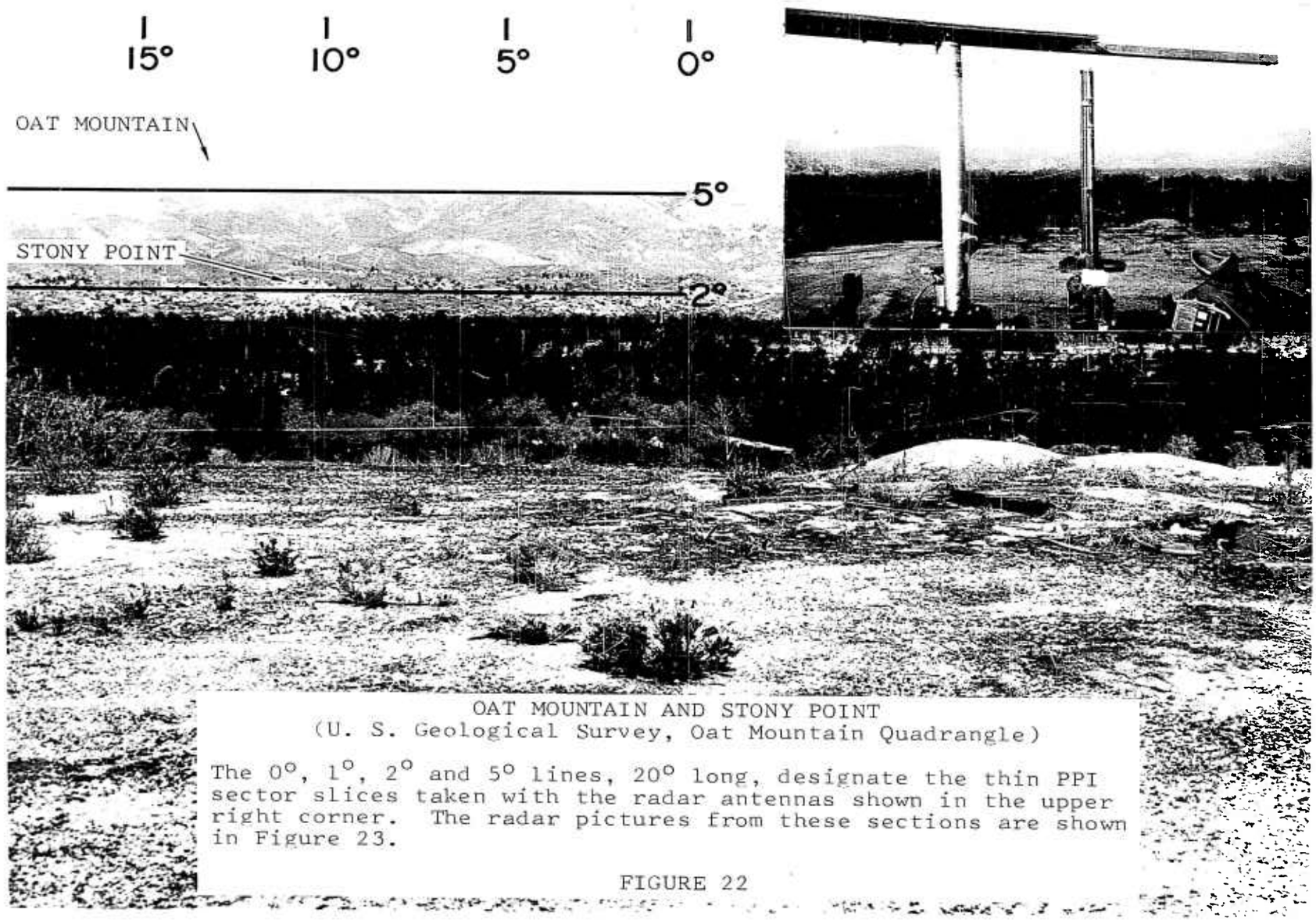

OAT MOUNTAIN AND STONY POINT
(U. S. Geological Survey, Oat Mountain Quadrangle)

The 0°, 1°, 2° and 5° lines, 20° long, designate the thin PPI sector slices taken with the radar antennas shown in the upper right corner. The radar pictures from these sections are shown in Figure 23.

FIGURE 22

ELEVATION INCREMENTS (0°, 1°, 2°) OF THIN (1° Elevation Beam)
PPI SECTORS (20°) WITH 0.35° AZIMUTH BEAM WIDTH

FREQUENCY: 16.2 KMC

THE RADAR SYSTEM TO PRODUCE THE 3-D DATA BELOW DID NOT USE STC OR TR TUBES. IF STC HAD BEEN AVAILABLE THE 3-D RESOLUTION WOULD HAVE BEEN FURTHER ACCENTUATED.

CROSSED BEAM 0.35° X 1° X 50 ft (PULSE WIDTH)

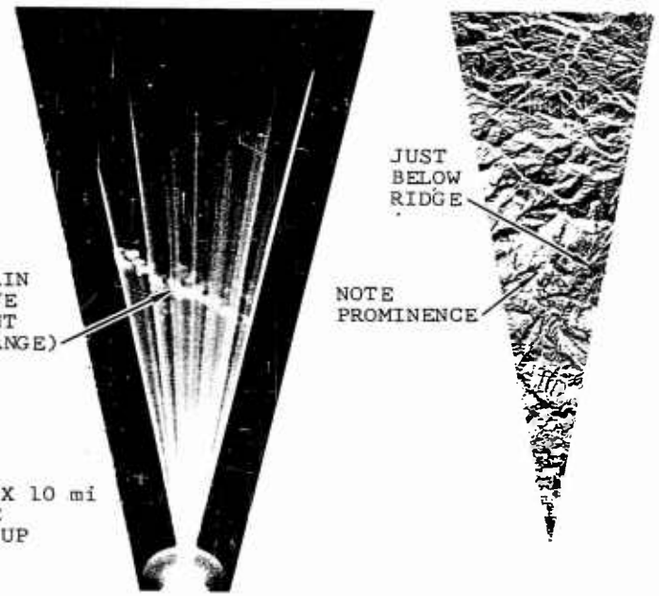

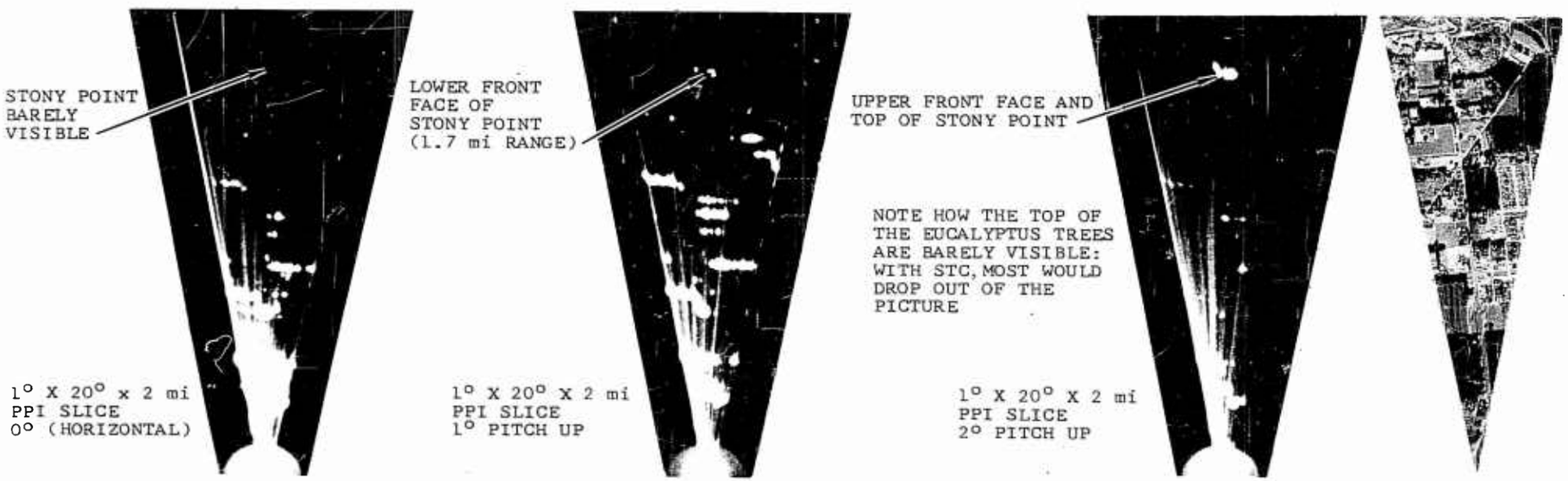

CROSSED BEAM 3D DISPLAY OF SENSOR OBSTACLE DETECTION DATA

FIGURE 23

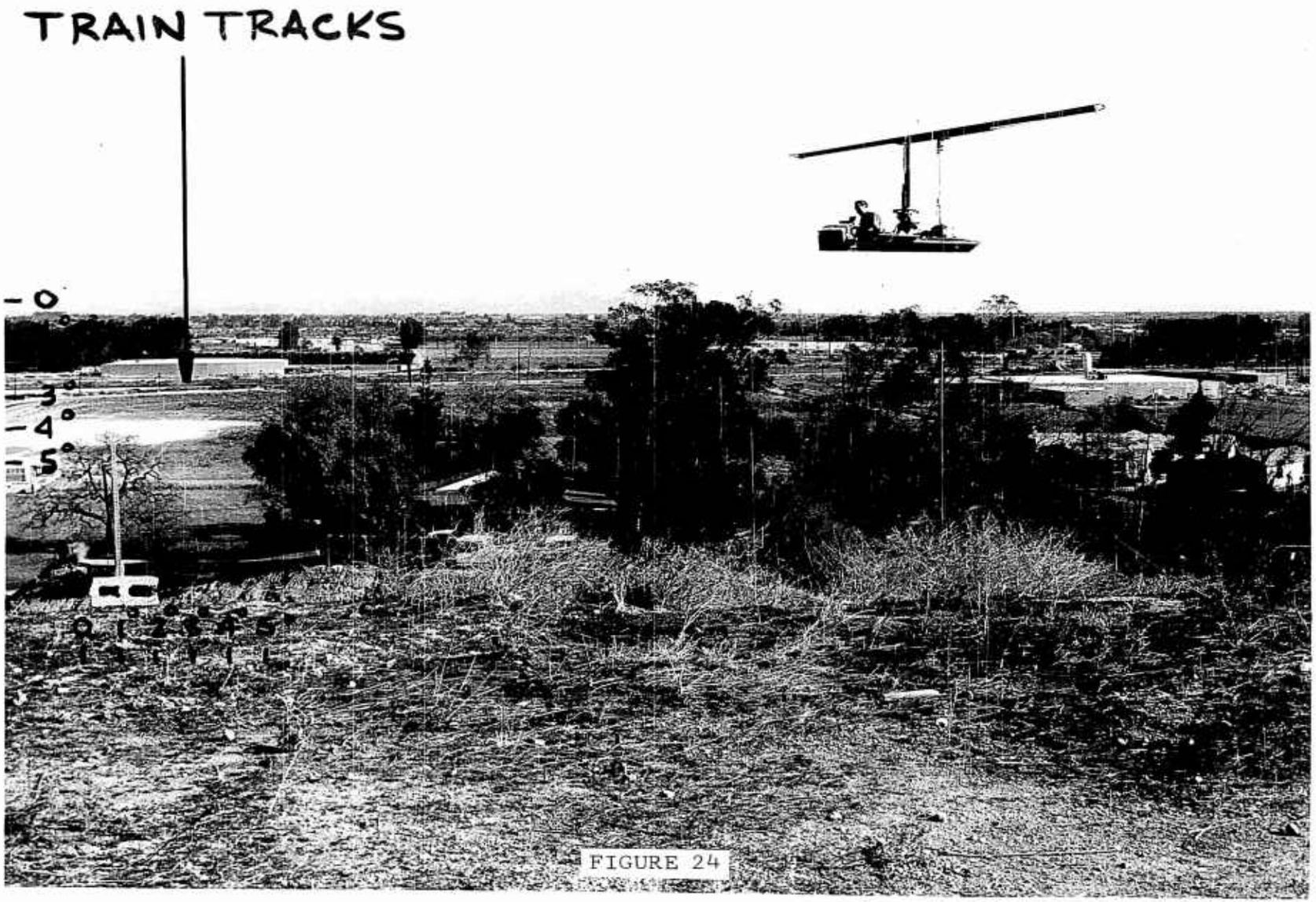

FIGURE 24

CROSS BEAM 3D SENSOR, OBSTACLE DETECTION DATA

FREQUENCY: 16.2 KMC

ELEVATION INCREMENTS OF THIN (1° ELEVATION BEAM) PPI SECTORS (20°) WITH 0.35° AZIMUTH BEAMWIDTH

THE RADAR SYSTEM TO PRODUCE THE 3D DATA BELOW DID NOT USE STC OR A TR TUBE. IF STC HAD BEEN INCORPORATED (IT WAS NOT AVAILABLE) THE CROSSED BEAM 0.35° X 50 ft 3D RESOLUTION WOULD HAVE BEEN FURTHER ACCENTUATED.

ELEVATIONS NOTED ARE FROM HORIZONTAL (0°)

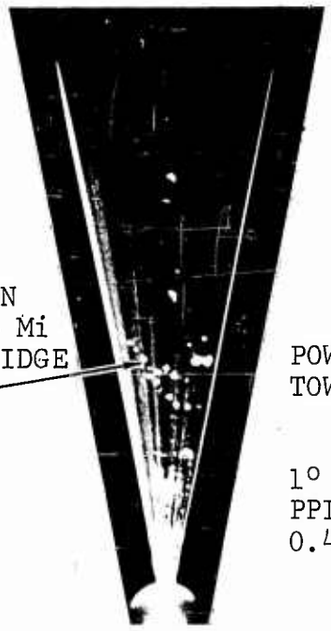

POWER TRANSMISSION TOWERS, RANGE ≈ 4 Mi (COMPARABLE TO BRIDGE SUPERSTRUCTURE)

1° X 20° X 10 Mi
PPI SLICE
0° (Horizontal)

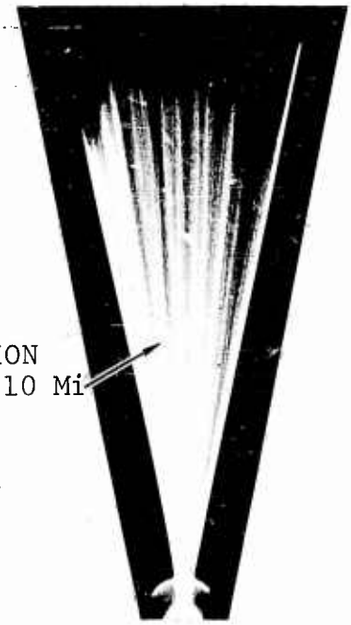

POWER TRANSMISSION TOWERS, RANGE ≈ 10 Mi

1° X 20° X 20 Mi
PPI SLICE
0.4° PITCH UP

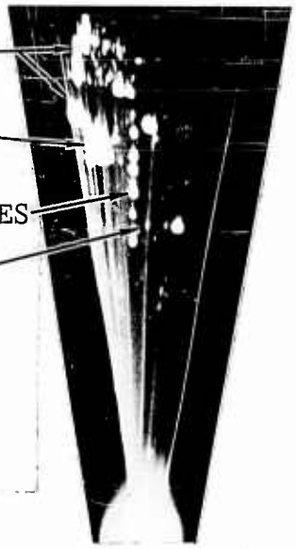

TREES

BUILDING

1.5 Ft DIA WOOD POLES

NO TRAIN

1° X 20° X 1 Mi
PPI SLICE
0° (Horizontal)

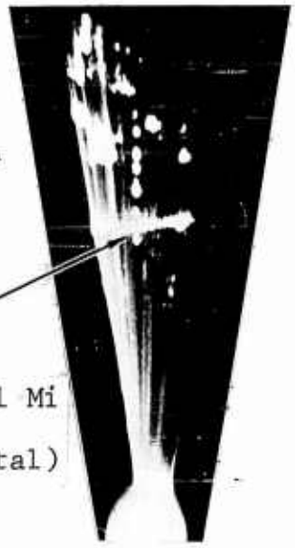

WITH TRAIN

1° X 20° X 1 Mi
PPI SLICE
0° (Horizontal)

FIGURE 25

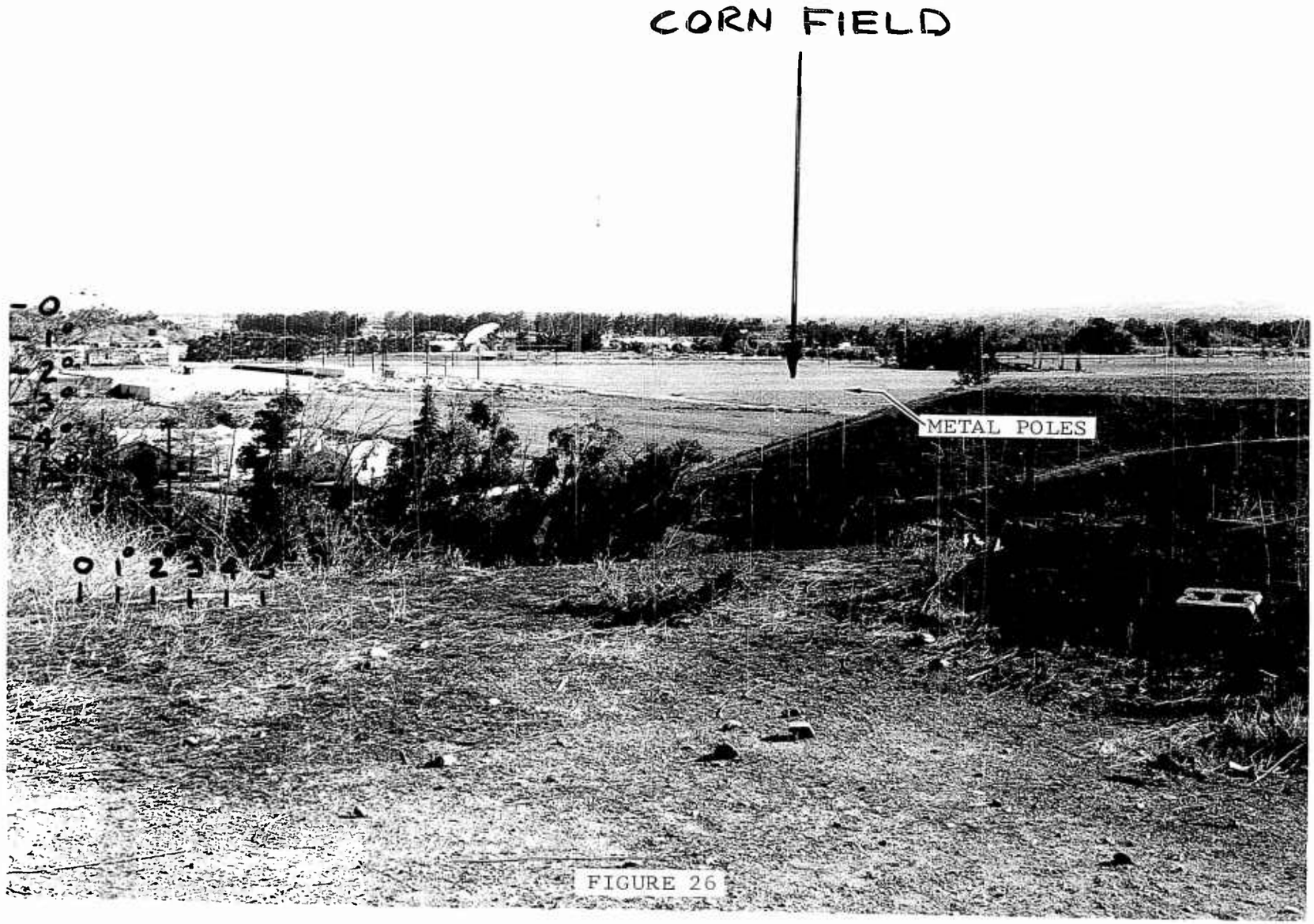

FIGURE 26

ELEVATION INCREMENTS (-0.5°, -1° Pitch Down) of THIN (1° Elevation Beam) PPI SECTORS (20°) WITH 0.35° AZIMUTH BEAM WIDTH

FREQUENCY: 16.2 KMC

THE RADAR SYSTEM TO PRODUCE THE 3D DATA BELOW DID NOT USE STC OR A TR TUBE. IF STC HAD BEEN INCORPORATED (IT WAS NOT AVAILABLE) THE CROSSED BEAM 0.35° X 1° X 50 ft 3D RESOLUTION WOULD HAVE BEEN FURTHER ACCENTUATED.

THE ELEVATION ANGLES NOTED ARE FROM HORIZONTAL (0°)

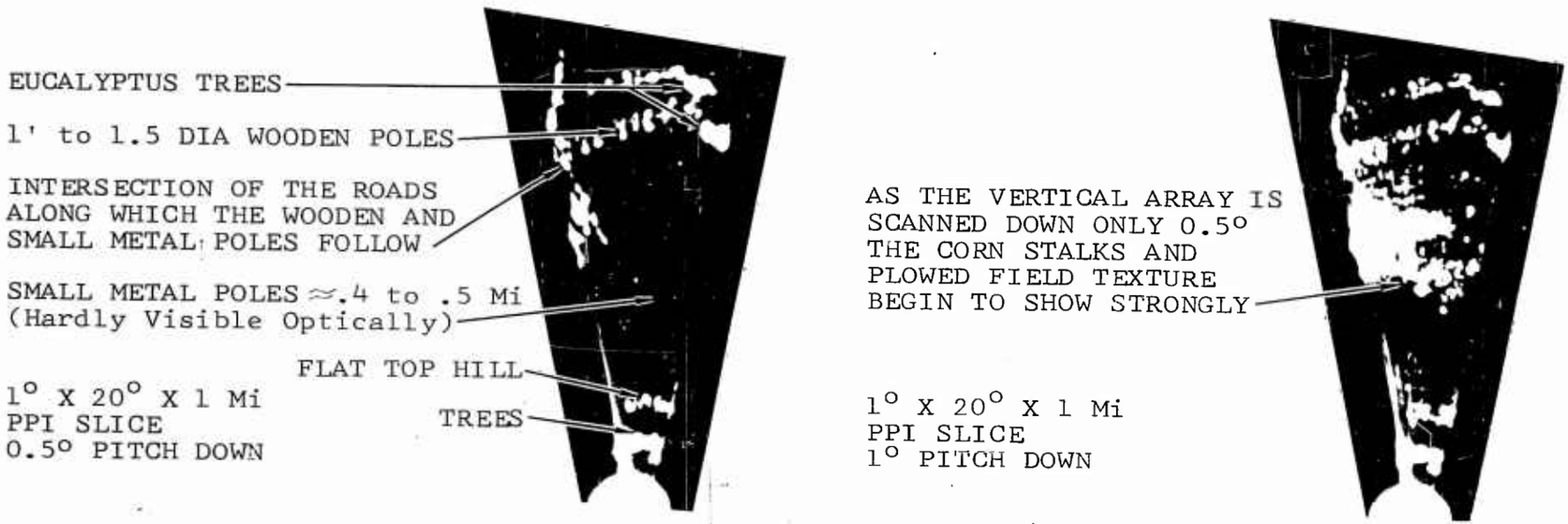

CROSSED BEAM 3D SENSOR, OBSTACLE DETECTION DATA

FIGURE 27

VIII. PERMANENT ARRAY INSTALLATION

After having proven in the early effort of this program that either a leading or trailing edge antenna would work equally well, and because the trailing edge antenna would require redesign of the trailing edge spar to produce a blade stressed for flight, it was decided to concentrate research on the leading edge configuration whereby regular production UH-1B blades could be easily modified to accept the rotor blade antenna without affecting the blade structurally.

Placement of the antenna array in the leading edge of the rotor blade was considered under the company-funded study conducted in early 1963. The idea was rejected at that time because of the erosion that occurs in the leading edge of the blade during rotation. A study of this erosion problem was conducted at Bell. Polyurethane and Neoprene exhibited the highest resistance to sand erosion of the non-metallic materials. Seventeen of the best eighteen materials were either Neoprene or Polyurethane compounds. Test results indicate that the best material tested was a Polyurethane compound by B. F. Goodrich Company designated as 3047A Estane. Samples of this and other Estane compounds were obtained and tested at microwave frequencies. B. F. Goodrich developed the composite Estane and Neoprene erosion boot which was used on the full length test blade.

The UH-1B main rotor blade has an aluminum box beam which is the leading edge structural member. To this is bonded the brass nose block which among other things, establishes the curvature of the leading edge. A thin layer of stainless steel is then bonded over the curved brass leading edge and extended down and over about 90 per cent of the box beam, serving as an erosion shield.

The radar antenna was installed in the leading edge of a used UH-1B rotor blade by cutting a slot .256 inches wide and .512 inches deep, the full length of the blade, extending through the stainless steel erosion shield and into the brass nose block. (See Figure 28) The slot had to follow the centerline of the leading edge and also parallel the axis of the blade chord. This requirement was made difficult by the .5 degree per foot twist built into the blade. A work aid using an air motor to drive an end mill "router" fashion was constructed. The work aid was designed to follow the centerline of the leading edge, with side guides to follow the blade twist. See Figure 29.

Tinning

To improve the bond between the copper waveguide antenna array and the brass nose block, the array was tinned using a cold wipe process. Step by step this procedure follows.

1. Remove grease and oils with a cloth dampened with a safety solvent. (Vythene was used.)

2. Remove light oxides with Scotch-Brite.

3. Wipe with Vythene.

4. Wipe with Metex acid tin solution to deposit a light tin coating.
5. Wipe with distilled water.

6. Dry.

Bonding

1. The machined slot in the blade was cleaned using Scotch-Brite and wiped with Vythene and a rag.

2. A layer of 3M EC2216 was brushed on the sides and bottom of the slot. A layer approximately .030 thick was deposited on bottom of slot.

3. Three lengths of No. 450-1/2 glass strands were embedded in the bottom of slot to give resiliency and shimming.

4. The array was placed in the slot. Templates made of 3/16 inch plexiglass cut out to conform to the leading edge curvature were used to position depth of array in slot. Working six inch intervals, the array was pushed down into position using the templates. Pieces of two inch wide mylar tape were placed over the leading edge to hold the antenna array in position during cure. Curing consisted of a 110 degree flash solvent for one hour, followed by 48 hours at room temperature. Preceding the bonding operation, a strip of .030 teflon was inserted in the array slit for protection against EC2216 squeeze out (Figures 30 and 31).

Erosion Boot

The composite erosion boot used to cover the leading edge of the blade consisted of three parallel strips of material making a total width of 7 inches. A strip of Estane 2.5 inches wide with the outer half inch of each edge tapered consituted the center or "window" section. On each side of the Estane, strips of Neoprene 2.75 inches wide with a half inch taper along one side and a long tapering feather edge on the other were used. The half inch tapered edges were overlapped and bonded, giving a uniform cross section thickness of .055 inches across the center four inches, the outer edges being feathered. (Figure 32)

This composite boot was used to satisfy the need for a low loss erosion material to cover the radiating window, together

with a high loss erosion material on either side of the window to suppress the back lobe as pointed out in Section IV. Goodrich Company is attempting to compound a one piece boot of Estane in which the center section will remain low loss, but outboard of the center, the Estane will be loaded with carbon to increase the losses. There was insufficient time remaining in the present program to complete compounding and testing (electrical and erosion) of an all Estane boot.

Installation of Boot on Rotor Blade

1. The leading edge of the rotor blade was cleaned, using Scotch-Brite and a Ketone wipe.

2. Goodrich A934B adhesion promoter applied to leading edge.

3. The Estane center section of the boot was masked.

4. The adjacent areas consisting of the Neoprene strips were spray coated with clear urethane adhesive.

5. The masking tape was removed from the center or Estane section of the boot and a double coat of EC 2126 applied to this area as well as the corresponding area of the blade.

6. The teflon protecting strip was removed from the antenna slit.

7. Estane section of boot was applied to center part of leading edge which had been previously coated with EC 2126.

8. Worked one side of blade at a time, starting from center of boot and working both inboard and outboard using Epon 934 epoxy adhesive, rolling to apply uniform pressure and provide squeeze out of air.

9. The boot was taped and held in position as work progressed.

10. Same procedure was applied to other side of blade. (See Figures 33, 34 and 35.)

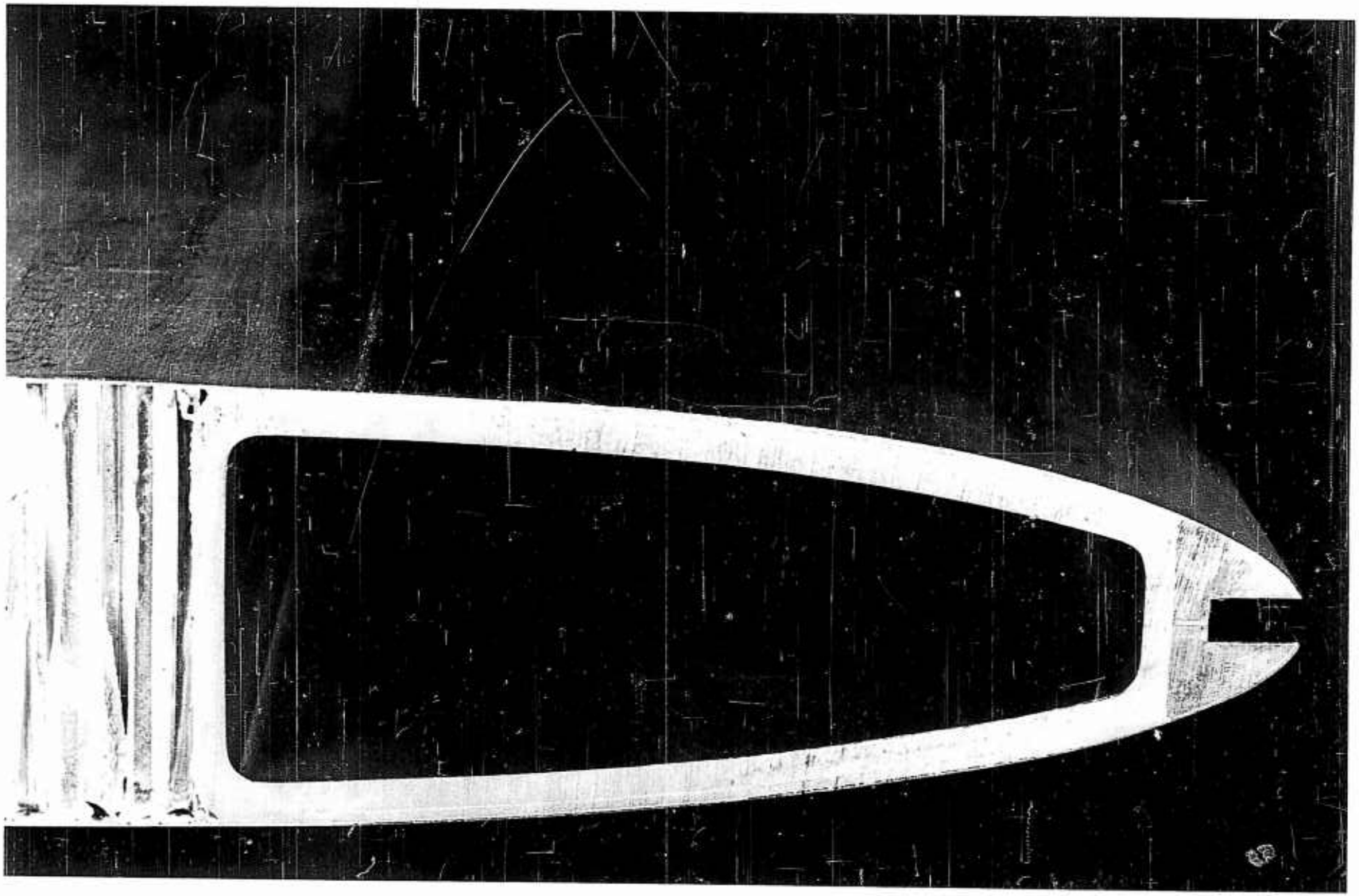

CROSS SECTION OF BLADE SHOWING ANTENNA SLOT

FIGURE 28

WORK AID USED TO CUT SLOT IN BLADE

FIGURE 29

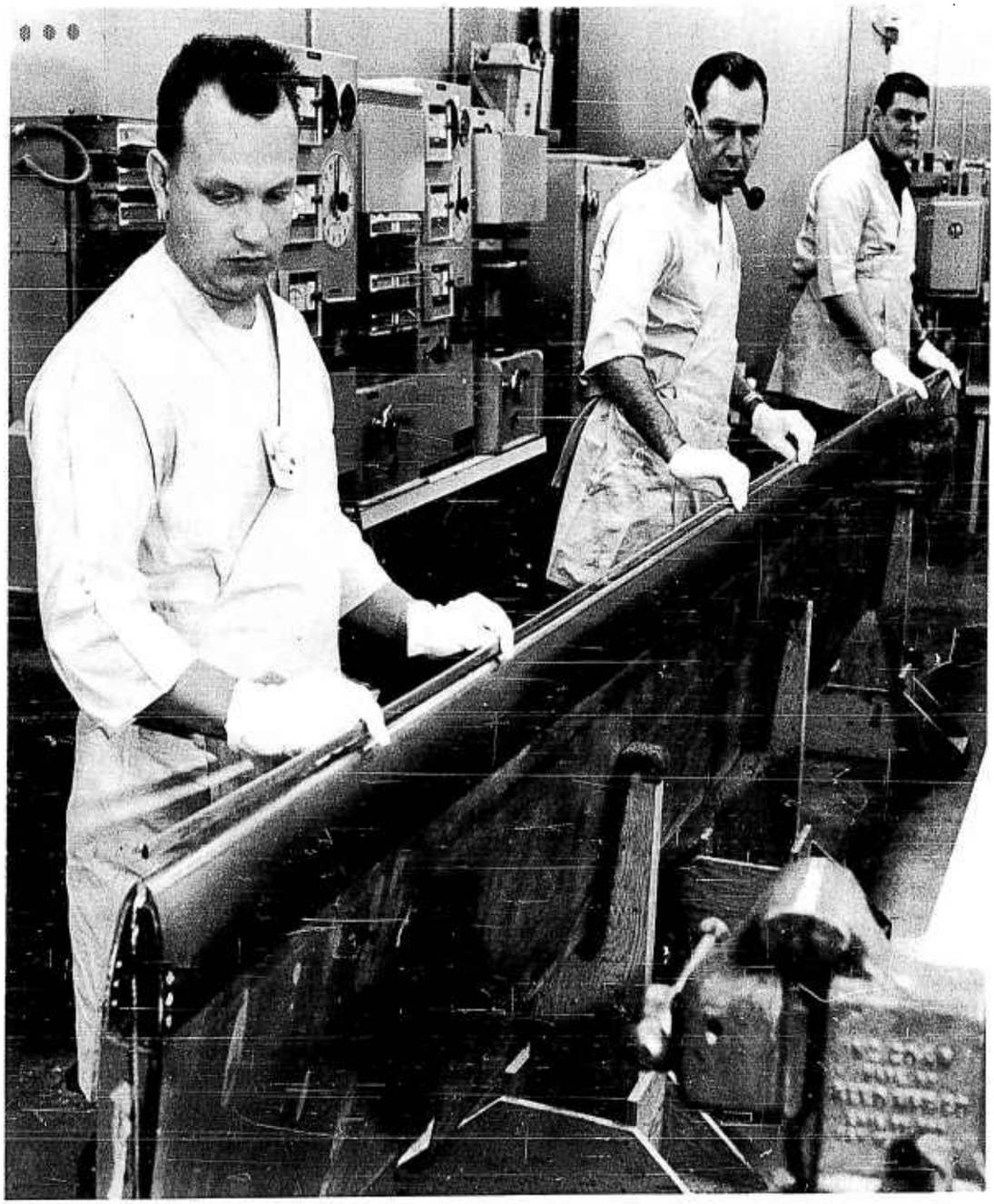

RADAR ANTENNA BEING INSTALLED IN LEADING EDGE SLOT

FIGURE 30

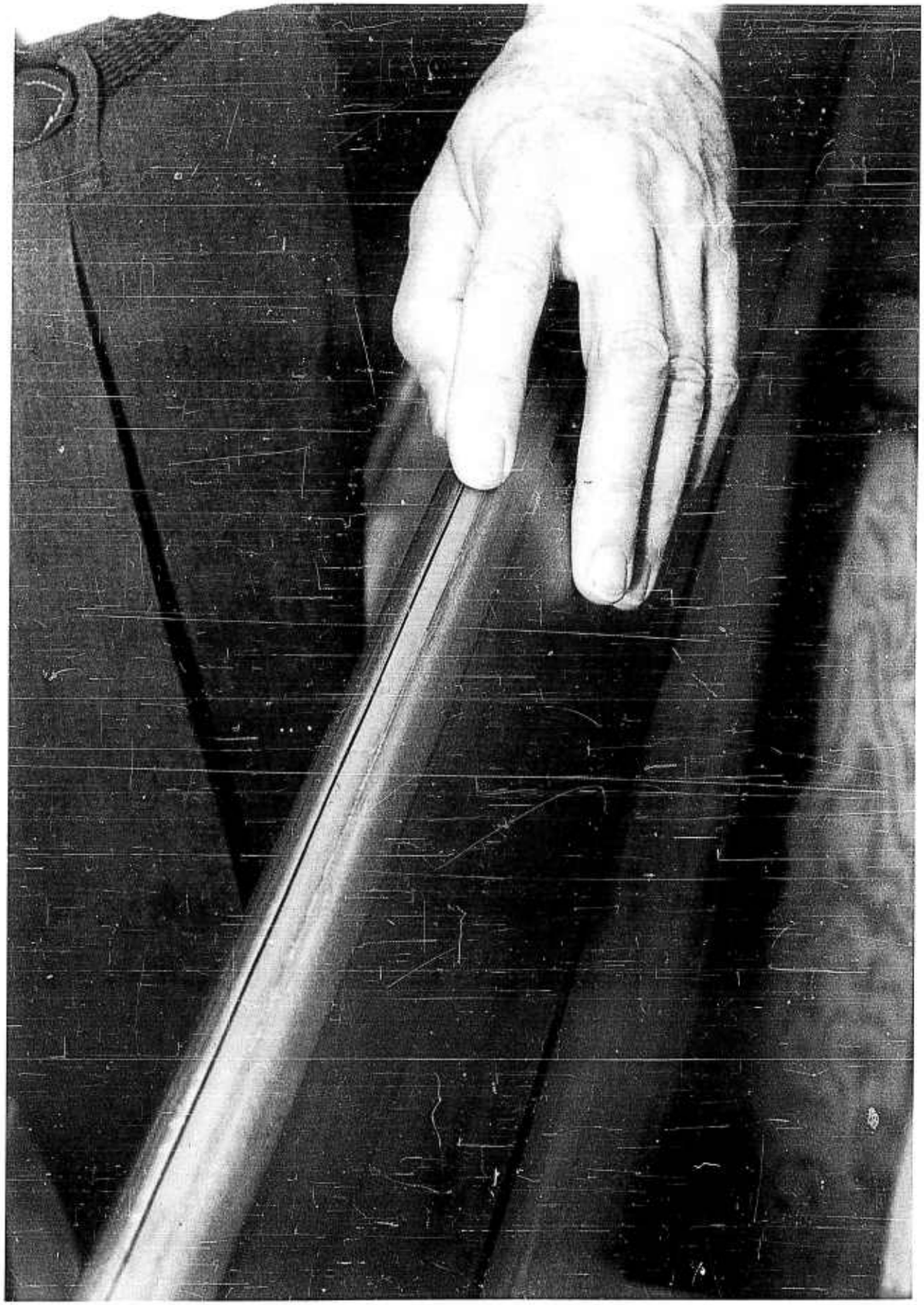

RADAR ANTENNA INSTALLED IN ROTOR BLADE

FIGURE 31

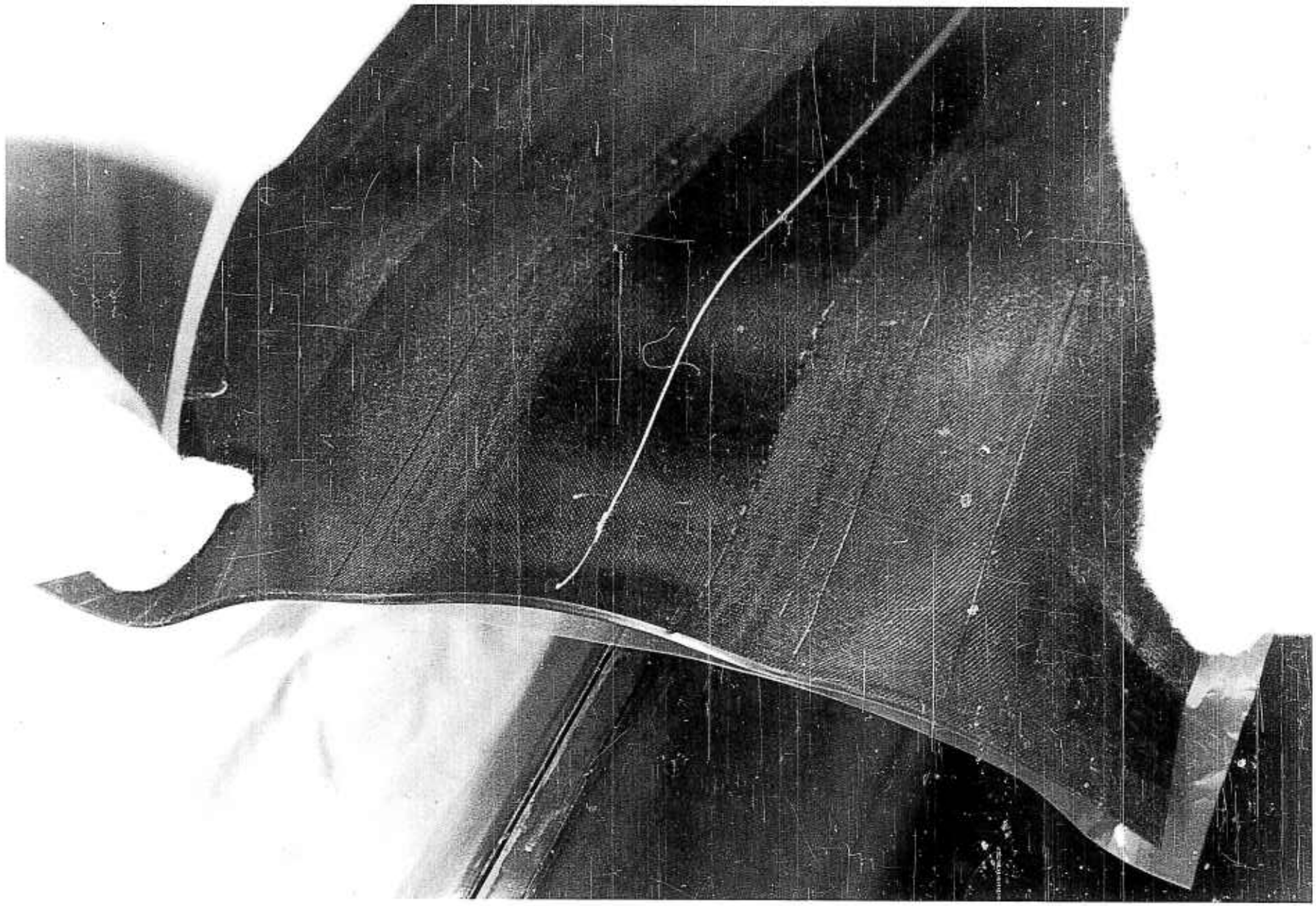

SPECIMEN OF COMPOSITE EROSION BOOT

FIGURE 32

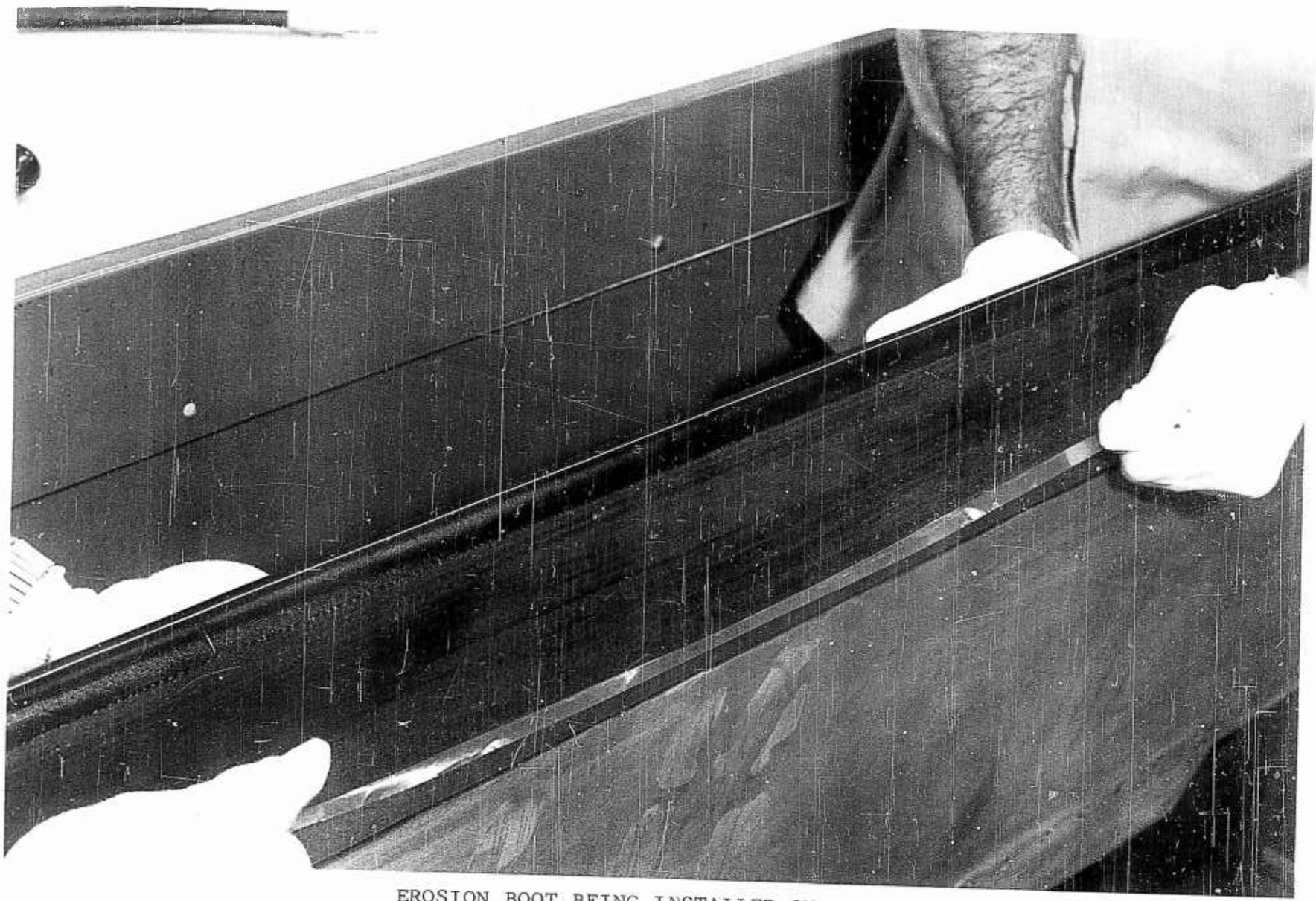

EROSION BOOT BEING INSTALLED ON BLADE

FIGURE 33

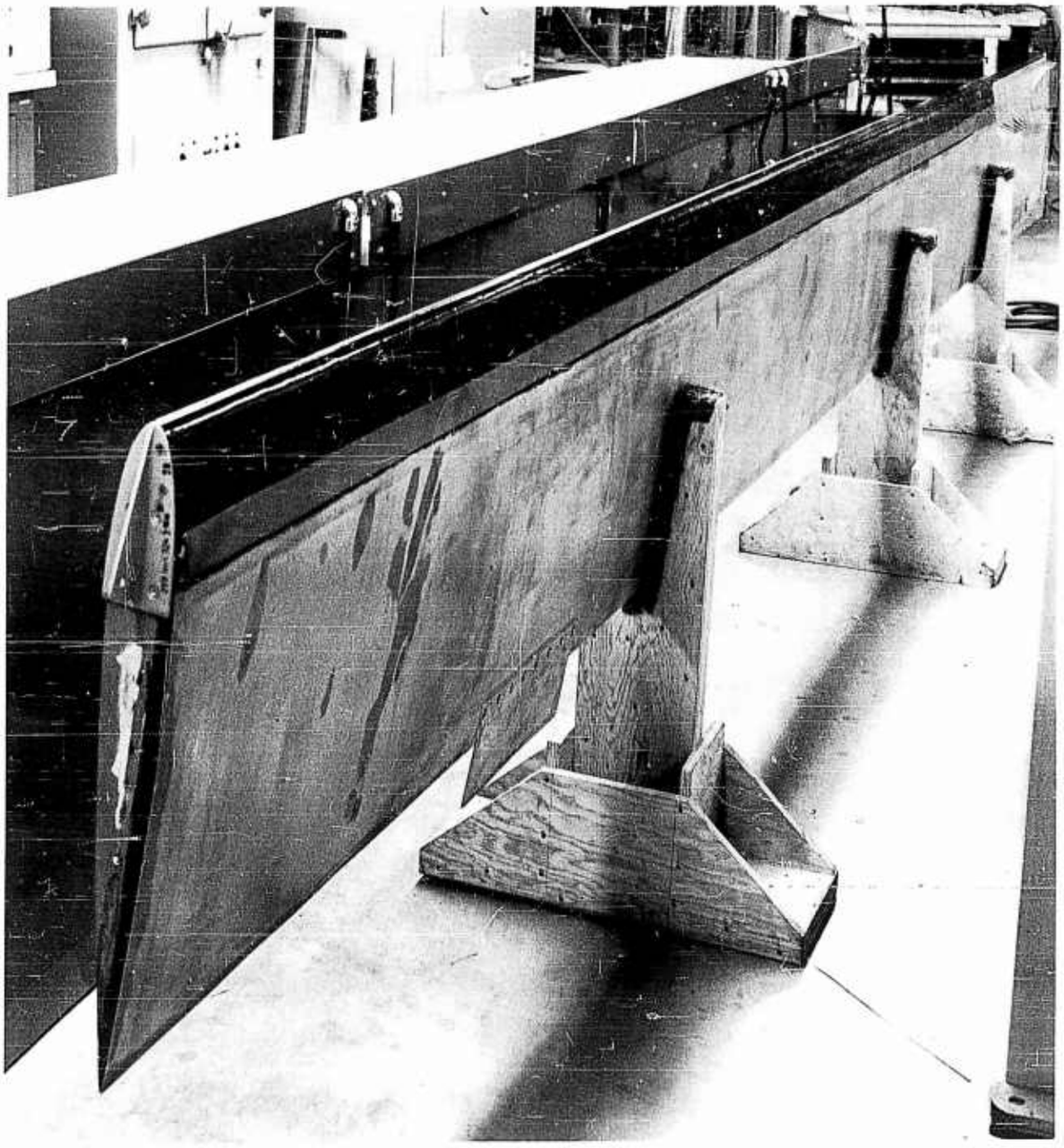

COMPLETED BLADE WITH RADAR ANTENNA AND EROSION BOOT INSTALLED

FIGURE 34

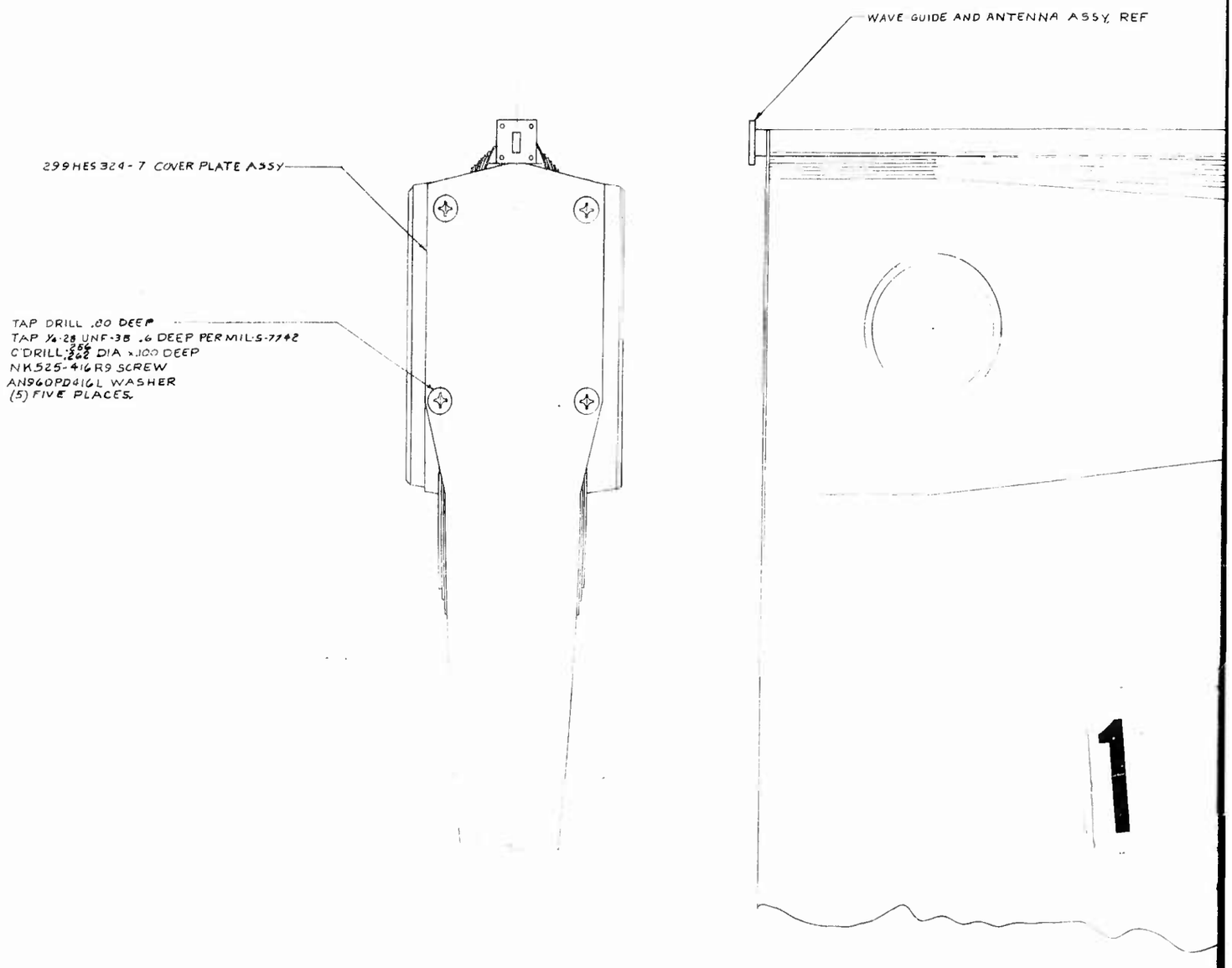
WAVE GUIDE AND ANTENNA ASSY, REF
299HES324-7 COVER PLATE ASSY
TAP DRILL .80 DEEP
TAP ¼-28 UNF-3B .6 DEEP PER MIL-S-7742
C'DRILL .252 DIA x.100 DEEP
NK525-416R9 SCREW
AN960PD416L WASHER
(5) FIVE PLACES.
1

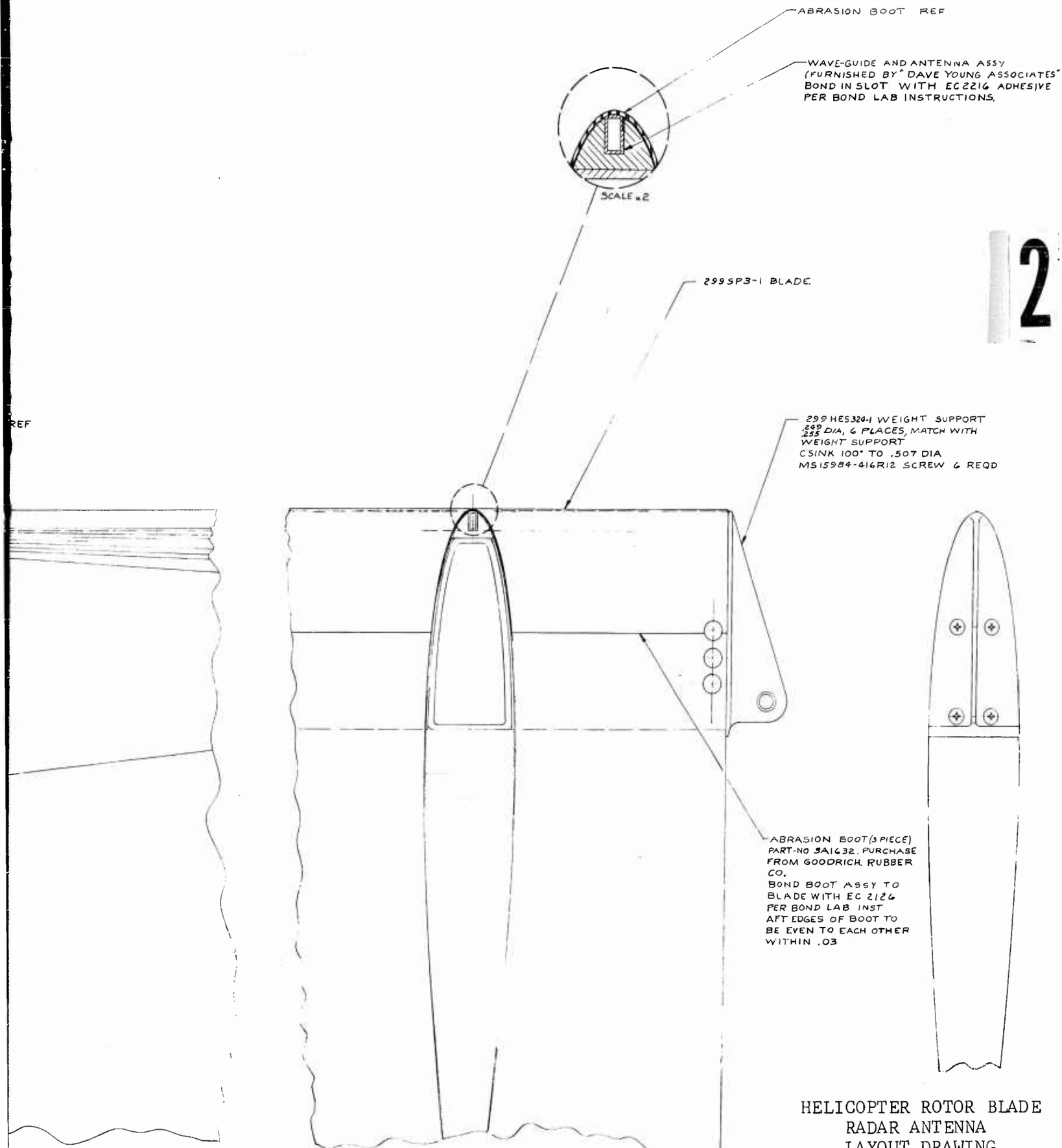

HELICOPTER ROTOR BLADE
RADAR ANTENNA
LAYOUT DRAWING

FIGURE 35

APPENDIX I

PPI DISPLAY

APPENDIX I

PPI DISPLAY

Timing, sweep and video circuits were provided to operate a standard commercial laboratory oscilloscope as a PPI indicator. A 541 Tektronix scope was used as the display device by using its internally generated sawtooth wave for the sweep and by using the CRT cathode circuit for intensity modulation. Since a linear pot was used rather than the usual sine cos functions, the scan sector was limited to about 20 degrees to keep distortion below 10 per cent. The timing control box is shown in Figure 36.

Sweep

The sweep for this display was obtained from the internally generated sawtooth waveform of the scope. The trigger circuit of the scope was set so that each time the transmitter was triggered the scope produced one sweep and then remained idle until the next transmitter trigger. The sawtooth waveform thus obtained was connected to a voltage divider which reduced its amplitude from about 150 volts to a usable level. This signal was impressed across a potentiometer physically connected to the gimbal mount of the Rotor Blade Antenna. The output of this potentiometer was directly proportional to the degree of rotation through which the antenna was rotated. This output was connected to the vertical amplifier of the scope and thus provided the second sweep necessary for a PPI sector scan. Small errors were expected to exist due to the potentiometer and the vertical amplifier. The potentiometer itself produced a slightly non-linear sweep due to the reactance of its winding. The vertical amplifier of the scope produced a propagation delay of 0.2 microseconds which is a range error of 100 feet. At the shortest range used (1 mile) this error is quite small and on the longest range (20 miles) became negligible. Another small error was introduced through use of the linear pot rather than the usual sine cos functions. The maximum error was about 8 per cent of full scale range.

Z-Axis Modulation (Intensity) and Video Amplifier

The video information was displayed by Z-axis modulation of the CRT. A video amplifier was designed and mounted inside the scope so that output leads would be as short as possible. The amplifier was basically the amplifier described in application note APP-27 of the Fairchild Semiconductor Division entitled "A 120 Volt 40 Nanosecond Transistor Video Amplifier". Many hours were spent adjusting the gain of the amplifier, the intensity control of the scope, and the settings of the scope camera for the best display of information. To acquire the correct resolution the spot size of the CRT should not have

exceeded approximately .017 of an inch. However, this is one-half the normal spot size which meant that the tube could never be turned on full if resolution were to be correct. This also meant that the video amplifier must provide signals that would operate the CRT at near cutoff and yet the CRT must provide enough light to record on film. The gain of the amplifier was first recorded. Then the amplifier was connected to the scope and tests were made to see what voltage pulse was needed to give the required 0.017 inch spot size.

Spot Size

Pictures were taken to give the same relative spot size on the negative (0.011 inch) as was viewed on the CRT. The values of the scope camera adjustments were found and recorded. The minimum signal that would appear on the film was then found and this then gave the dynamic range of Z-axis information. This was approximately 15 db of input signal.

The intensity knob of the 541A oscilloscope had to be replaced with a digital vernier knob for better control. Full range of the intensity control was 00.0 to 85.0 on the vernier knob. Visually, a spot (signal pulse width was less than 0.017 inches) was just detectable at an intensity setting of 71.7 and would almost bloom at 73.0. For a line (full width of scope face) the setting became 45.7 to just be detectable and 47.2 to almost bloom. Using a .1 microsecond pulse width the intensity setting and pulse amplitude combination was investigated using polaroid type 47 film as a detector. For values of pulse amplitude expected from the radar receiver it was found that for one second exposure at an "f" setting of 5.6 on the camera and an intensity setting of 47.5 on the scope the following data was recorded.

Rec. Input in D.B.M.	Rec. Output In Volts	Video Ampl. Output In Volts	Spot Size in Inches Vert.	Horiz.
-20	0.06	1.0	.005	.010
-11	0.13	2.2	.016	.022
- 4	0.185	3.2	.025	.025
+10	0.3	5.5	.029	.030
?	0.5	9.5	.32 (Phosphor Saturated)	.024
			Blooms beyond this size	

All of the above information was based upon constant speed of rotation of the antenna but the antenna was turned manually, which proved to be much slower during the field test than in the laboratory. This caused the film in some cases to be over exposed and produced spot sizes well in excess of the 0.011 inches optimum, but the PPI radar data was still reasonably effective due to the high resolution of the antennas.

S.T.C. Circuit

The S.T.C. circuit controls (see schematic) the conductance of microwave switching diodes causing the radar return to be attenuated in the waveguide before it reaches the receiver. While the circuit was not used on the radar, the design details of development are reported. This circuit consists of a switch circuit, a current ramp circuit, a back bias circuit and the microwave diodes and their mount. The diodes do not attenuate the signal when forward biased (conducting) but as the bias is changed to a back bias condition the diodes switch and a large attenuation of the signal is achieved. This action is explained in an article entitled "Microwave Diodes for Switching and Modulating" published in the December 1963 issue of Special Report on Electronics. The switch circuit is used to start the current ramp of the current ramp circuit which provides the forward bias current for the diodes. At the time this current ramp starts the diodes are back biased and therefore the ramp has no effect until the back bias falls to zero. To remove the back bias the input signal shuts off the back bias circuit and its voltage starts to fall. The actual curves of the back bias fall time and of the current ramp are controlled so as to give a composite curve. This composite curve impresses a current-voltage wave shape on the diodes which cause them to vary their attenuation so that short range returns are attenuated more than long range returns. The ideal relationship is found when the signal return from a specific target is the same amplitude (at the receiver input) for all range values under consideration. Timing was critical for this circuit since the attenuation must change at a given rate from a given time related to the transmitter firing time. The S.T.C. circuit needs a pre-trigger which was not available during the field tests to be effective and without this pre-trigger the circuit caused too much attenuation of the received signals at short range settings. For range settings of 5 miles and over, the S.T.C. would only suppress the near targets and therefore would not substantially improve the PPI simulated display. It was decided during the field tests that the use of the S.T.C. circuit would not justify the time necessary to insert the circuit into the system.

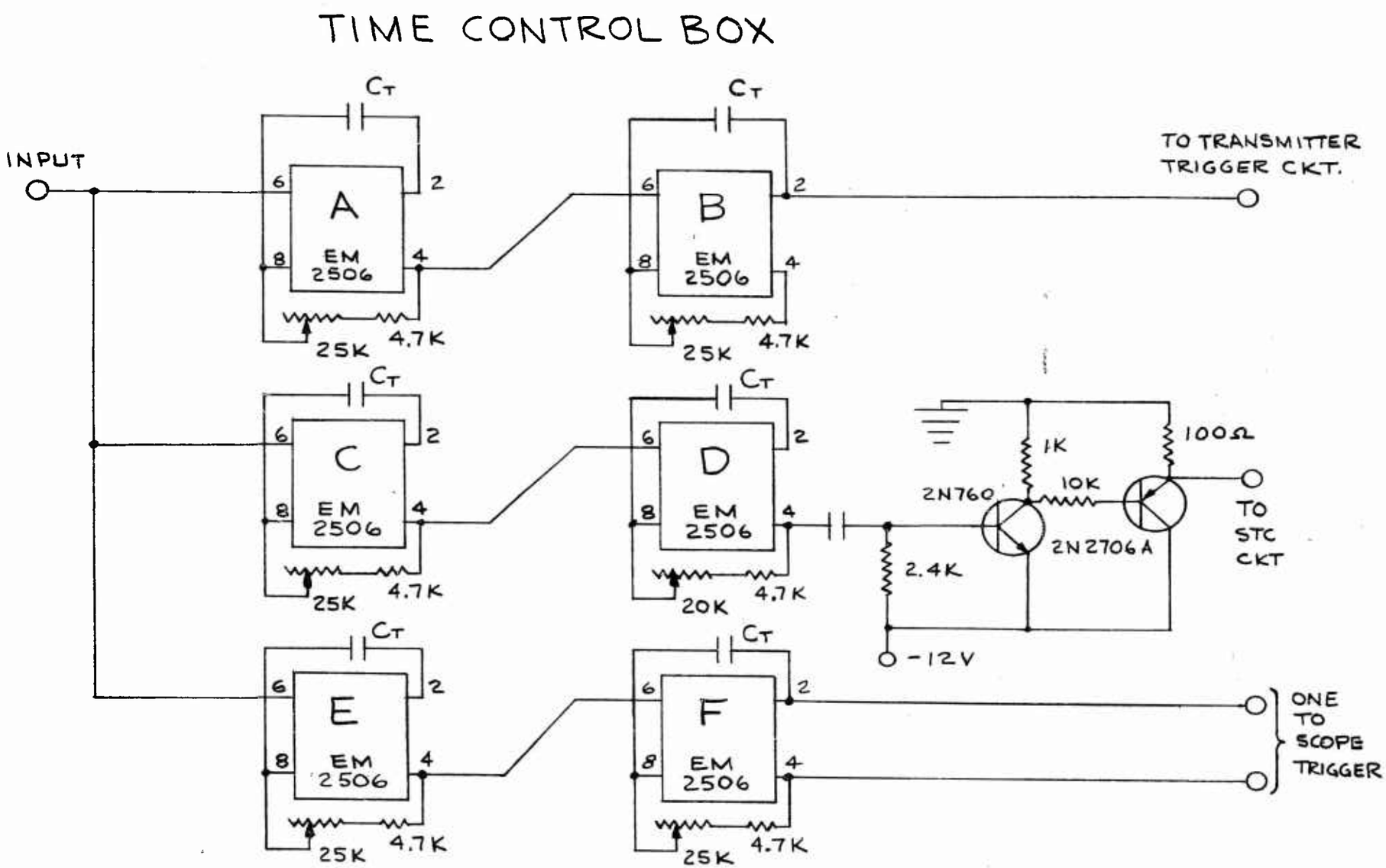
TIME CONTROL BOX
INPUT
C_T
A
B
C
D
E
F
EM 2506
6
2
8
4
25K
4.7K
20K
TO TRANSMITTER TRIGGER CKT.
1K
100Ω
10K
2N760
2N2706A
2.4K
-12V
TO STC CKT
ONE TO SCOPE TRIGGER

FIGURE 36

MONOSTABLE MULTIVIBRATOR

(1 circuit per module)

The "Single Shot" is designed to provide a source of pulses for the system clock and special reset functions, or time delays. It will provide positive and negative outputs the duration of which will depend on the application. Included in the module is a three term (2 level & 1 pulse) AND Gate to the trigger input. The pulse width can be trimmed or lengthened by inserting additional external capacitance between terminals 8 and 2. The standard delay is 1 microsecond ± 20% and other delays are available on request.

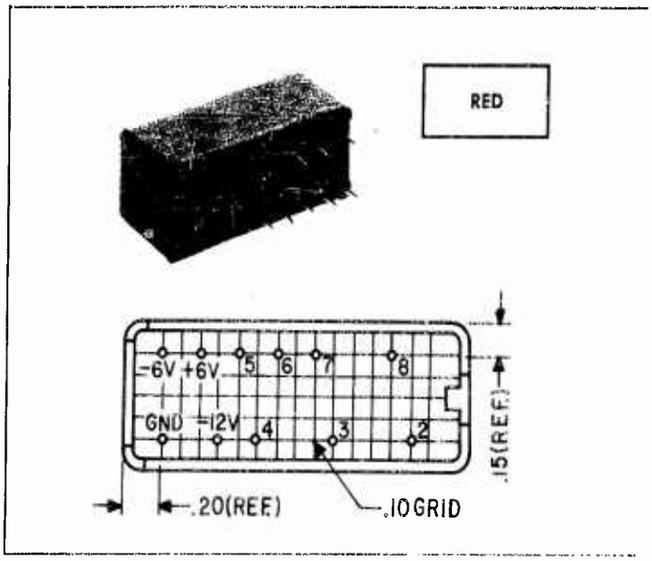

ELECTRICAL SPECIFICATIONS

INPUT

Pulse

Amplitude	5.5 to 6 volts positive
Rise Time	0.20 microsecond maximum
Maximum Clock Rate	Dependent on output pulse width—250 kcps max for pulses of less than three microsecond duration.

Level

Disable Gate	−5.6 to −6.5
Enable Gate	−0.2 to +0.3 volts
Gate setup time	2 microseconds max.

OUTPUT

Voltage

Conducting (Logical "1")	0 to −0.2 volts
Non Conducting (Logical "0")	−6 to −6.5 volts

Duration

For Pulse Generation	1 microseconds ±20%

Transient Times (Fully Loaded)

Delay	0.18 microsecond
Rise	0.30 microsecond
Storage	0.10 microsecond
Fall	1.00 microsecond

LOADING

See Loading Chart

POWER REQUIREMENTS

−12 volts ±5%	−18 ma
−6 volts ±5%	+ 6 ma
+6 volts ±5%	+0.6 ma

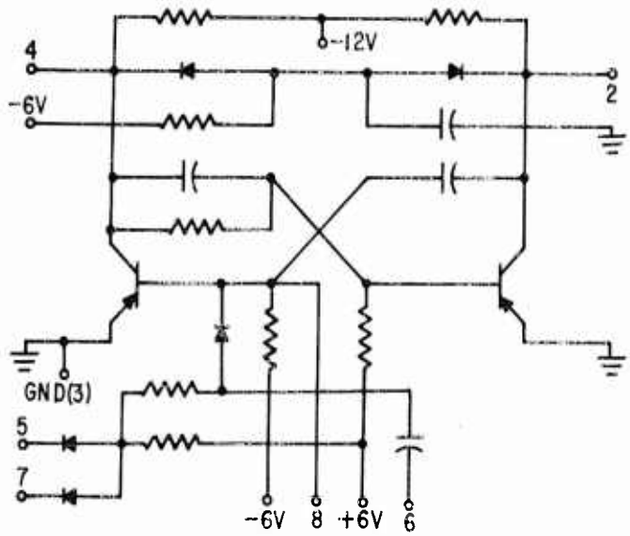

(See reverse side for Mechanical Specifications)

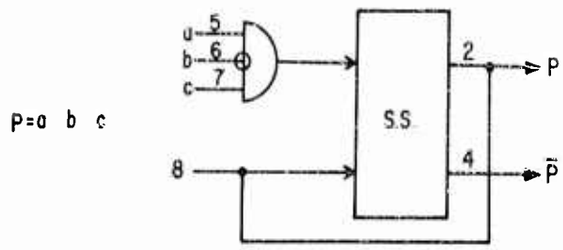

ELECTRONIC MODULES CORPORATION
EMC
CLearbrook 2 2900
1949 GREENSPRING DRIVE · TIMONIUM, MARYLAND

FIGURE 37

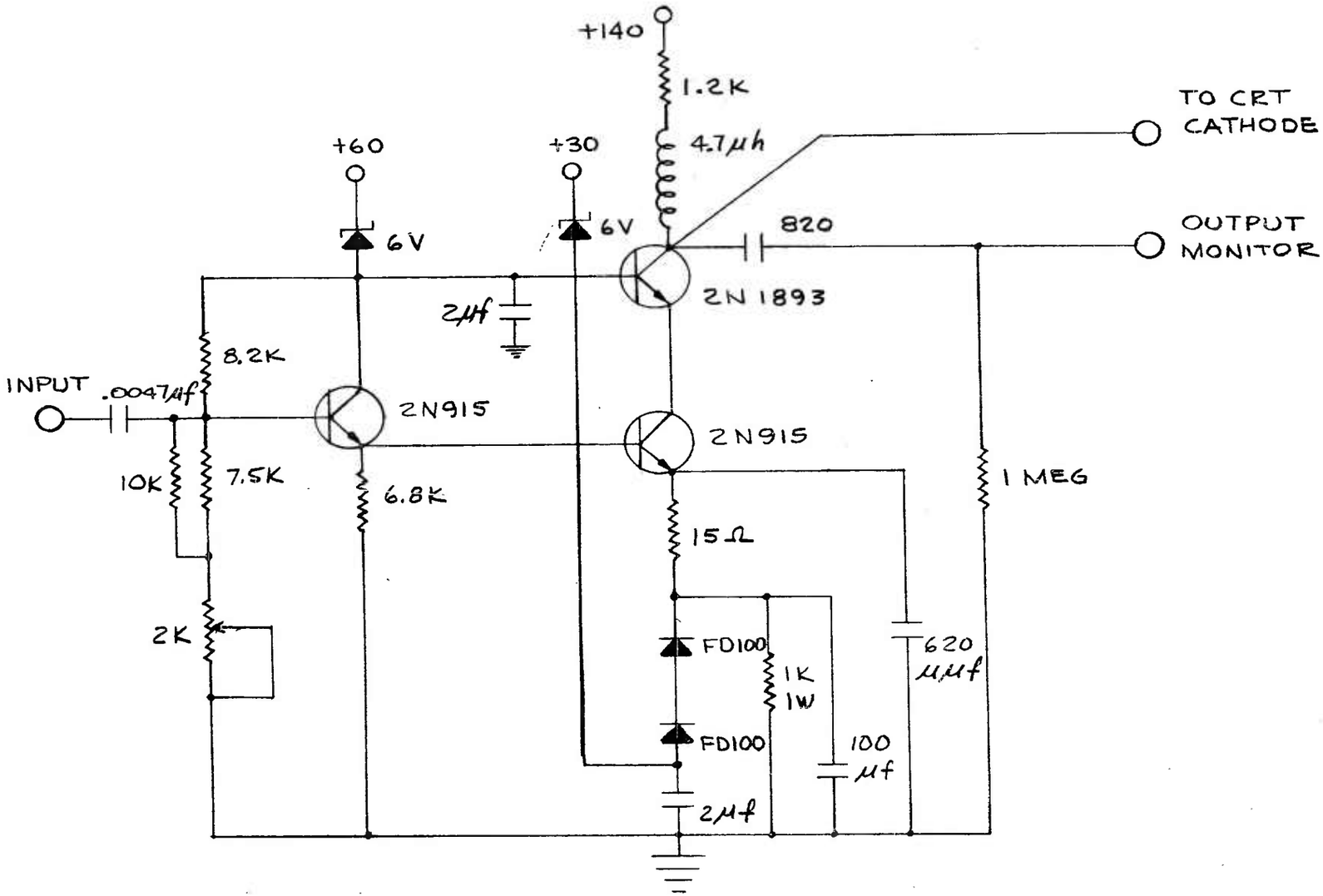

FIGURE 38

11/14/64 AHL	VIDEO AMPLIFIER

VIDEO AMPLIFIER VOLTAGE REGULATORS

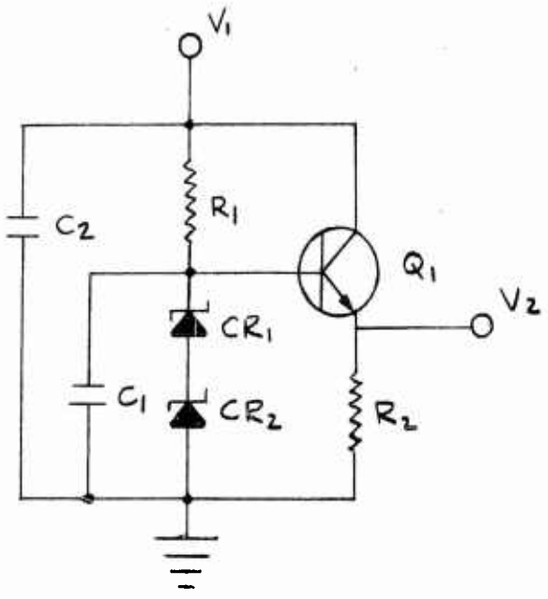

V_1	30	60	140
V_2	45	76.5	181.5
R_1	5.1K	5.6K	91K
R_2	62K	12K	120K
CR_1	¼M30Z5	¼M30Z5	¼M140Z5
CR_2	———	¼M30Z5	———
Q_1	2N1893	2N1893	HD81HB
C_1	50MFD 50 V	20MFD 100 V	50MFD 150 V
C_2	50MFD 50 V	20MFD 100 V	50MFD 150 V

FIGURE 39

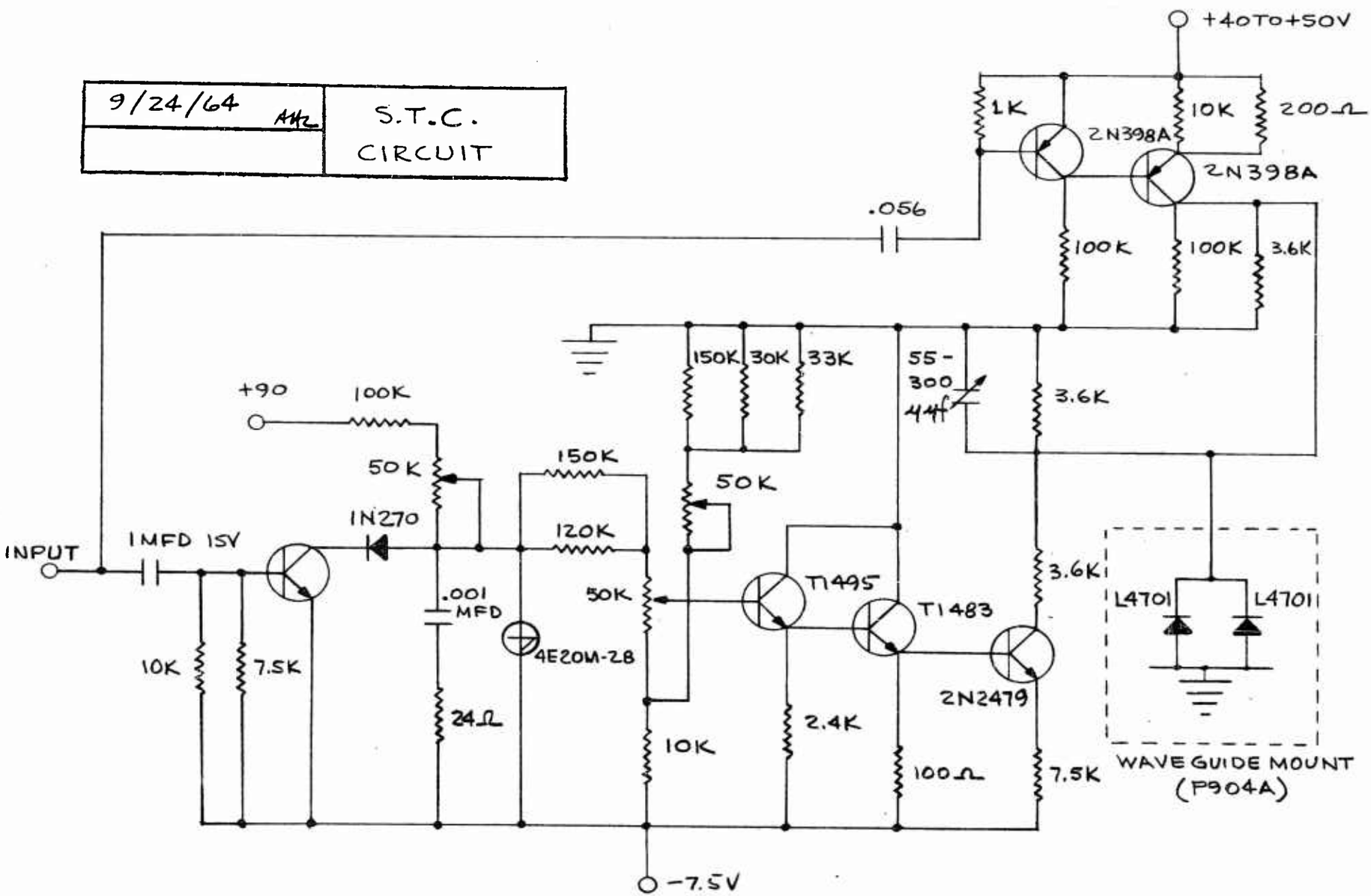
9/24/64 AHL
S.T.C.
CIRCUIT
+40TO+50V
1K
2N398A
10K
200Ω
2N398A
.056
100K
100K
3.6K
150K
30K
33K
55 - 300 44f
3.6K
+90
100K
50K
150K
50K
IN270
120K
INPUT
1MFD 15V
.001 MFD
4E20M-28
50K
T1495
T1483
3.6K
L4701
L4701
10K
7.5K
24Ω
2N2479
2.4K
10K
100Ω
7.5K
WAVE GUIDE MOUNT (P904A)
-7.5V

FIGURE 40

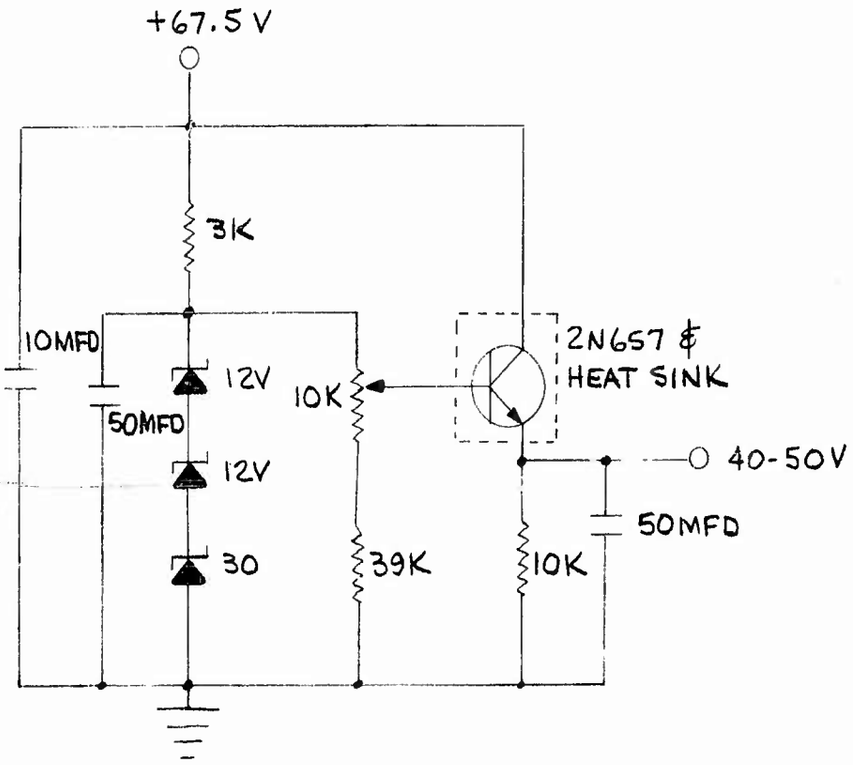

STC CIRCUIT
VOLTAGE
REGULATOR

FIGURE 41

REFERENCES

1. Lindenmeyer, Leonard and Young, David W., Rotor Blade Radar Antenna, Phase I. Bell Helicopter Company Technical Report No. 299-099-251, Prepared for the Office of Naval Research under Contract Nonr 4148(00), January, 1965.

2. Young, David W., JANAIR Crossed Beam Radar Project. David W. Young and Associates, Inc. Interim Report, ASTIA No. AD 435 558, June 1964.

3. Young, David W., High Speed, Raster Scanning, High Resolution, Radar Sensor for Vertical Display. Prepared for JANAIR, under Contract Nonr 4032(00) by David W. Young and Associates, Inc., July 30, 1964.

JANAIR DISTRIBUTION LIST

CDR W.A. Engdahl (RAAV-9)
Chief, Bureau of Naval Weapons
Room 1W98, W Building
Washington, D.C. (3)

Mr. Henry Birmingham
U. S. Naval Research Laboratory
Washington, D.C.

Mr. L. S. Guarino
Airborne Instrument Laboratory
Commanding Officer
U.S. Naval Air Development Center
Johnsville, Pennsylvania

Commanding Officer
Office of Naval Research Br. Office
495 Summer Street
Boston, Massachusetts

Commanding Officer
Office of Naval Research Br. Office
219 S. Dearborn Street
Chicago, Illinois 60604

Commanding Officer
Office of Naval Research Br. Office
1030 East Green Street
Pasadena 1, California

LCDR J. Charles
Life Sciences Department
Point Mugu, California

Headquarters
Ministry of Aviation
Saint Giles Court
London, EC-2, England

ODDR&E Office of Electronics
Attn: CDR W.W. Vallandingham, USN
Pentagon (Room 3D1037)
Washington, D.C.

Commanding Officer
Office of Naval Research Br. Office
Box 39, Navy #100, Fleet P. Office
New York, New York

Commanding Officer
Office of Naval Research Br.
Office
207 West 24th Street
New York 11, New York

Commanding Officer
Office of Naval Research Br.
Office
1000 Geary Street
San Francisco 9, California

Federal Aviation Agency
Information Retrieval (MS-112)
Washington, D.C.

Commander
Hdqtrs., Air Force Systems Command
Andrews AFB, Maryland

Commandant
School of Aviation Medicine, USAF
Attn: Research Secretariat
Randolph AFB, Texas

Chief, Engr. Electronics Section
National Bureau of Standards
Washington, D.C.

U.S. Naval Training Devices Center
Attn: Joe N. Pecoraro
Head, Equip. Res. Div.
Pt. Washington, L.I., N.Y.

Hqs., Quartermaster R&E Command
Quartermaster, R&D Center
Natick, Massachusetts

Defense Documentation Center
Cameron Station
Alexandria, Virginia (20)

British Defense Research
P. O. Box 680
Benjamin Franklin Station
Washington, D.C. (2)

Defense Research Member
Canadian Joint Staff
2450 Massachusetts Ave., N.W.
Washington, D.C. (2)

National Aeronautics & Space
Administration
1520 H Street, N.W.
Code RBB
Attn: Mr. Lowell Anderson
Washington, D.C.

CAPT John D. Kuser, USN
Office of Naval Research
Air Programs, Code 461
Room 4231, Main Navy
Washington, D.C.

AFFDL (FDC)
LCOL. L.C. Wright
Wright-Patterson Air
Force Base, Ohio (2)

Headquarters
USAF (AFRSTB)
MAJ W. Hipple
Washington, D.C. (2)

National Aeronautics & Space
Administration
1520 H Street
Attn: Bertram A. Mulcahy, Chief
Division of Research

Director
Naval Research Laboratory
Attn: Tech. Info. Office
Washington, D.C.

Headquarters
RTD (RTNF)
MAJ. C.R. Wheaton
Bolling Air Force Base
Washington, D.C.

Staff Officer Medical (IAM)
RAF Staff, British Embassy
3100 Massachusetts Avenue
Washington, D.C.

Raymond F. Bohling
Code REC
NASA Headquarters
Washington, D.C. 20545

Civil Aeromedical Research Institute
Federal Aviation Agency
Aeronautical Center
P. O. Box 1082
Oklahoma City, Oklahoma 73101

U.S. Army
Human Engineering Laboratories
Aberdeen Proving Ground
Attn: Mr. R. Cassatt
Maryland 21005

Mr. Carmine Castellono
Code 3101
Naval Training Devices Center
Pt. Washington, L.I., N.Y.

Commanding Officer
USAEL
Attn: AMSEL-RD-SRI
Mr. B. S. Gurman
Ft. Monmouth, New Jersey

Commanding Officer
USAEL
Attn: AMSEL-RD-SRI
Mr. T.E. Maloney
Ft. Monmouth, New Jersey

Commanding Officer
USAEL
Attn: AMSEL-RD-SRI
Mr. S.J. Zywotow
Ft. Monmouth, New Jersey

Commanding Officer
USAEL
Attn: AMSEL-RD-SS
Ft. Monmouth, New Jersey

Commanding Officer
USAEL
Attn: AMSEL-RD-S
Mr. L. E. Evenson

JANAIR DISTRIBUTION LIST CONT'D

Commanding Officer
USAEL
Attn: AMSEL-AV
Headquarters
USAECOM
Fort Monmouth, New Jersey

Commanding Officer
USAMC Headquarters
Attn: AMCRD-DE-S
Mr. W. Cary Robinson
Washington, D.C.

Commanding Officer
USAMC Headquarters
Attn: AMCRD-AFS
Washington, D.C.

Chief of Research & Development
Department of the Army
Attn: CRD/R
Lt.Col. A.B. Shattuck
Washington, D.C.

Mr. John Grey
Aviation Test Board
Ft. Rucker, Alabama

Commanding Officer
USAMC Headquarters
Attn: AMCRD-R
Washington, D.C.

Commanding Officer
USAMC Headquarters
Attn: AMCRD-D
Washington, D.C.

Commanding Officer
USAMC Headquarters
Attn: AMCRD-DM
Washington, D.C.

Commanding Officer
USAMC Headquarters
Attn: AMCRD-S
Dr. Crenshaw
Washington, D.C.

Commanding Officer
U.S. Army Combat Develop. Command
Lt.Col. J.P. Smith
Ft. Belvoir, Virginia 22060

Royal Aircraft Establishment
Farnborough, Hants
England

Unclassified

Security Classification

DOCUMENT CONTROL DATA - R&D

(Security classification of title, body of abstract and indexing annotation must be entered when the overall report is classified)

1. ORIGINATING ACTIVITY *(Corporate author)*

Bell Helicopter Company
P. O. Box 482, Fort Worth, Texas 76101

2a. REPORT SECURITY CLASSIFICATION

Unclassified

2b. GROUP

3. REPORT TITLE

Rotor Blade Radar Antenna - Phase II

4. DESCRIPTIVE NOTES *(Type of report and inclusive dates)*

Interim Final Report

5. AUTHOR(S) *(Last name, first name, initial)*

Palmer, James E.
Young, David W.

6. REPORT DATE	7a. TOTAL NO. OF PAGES	7b. NO. OF REFS
February 1965	64	3

8a. CONTRACT OR GRANT NO.	9a. ORIGINATOR'S REPORT NUMBER(S)
Nonr 4148(00)	BHC No. 299-099-275
b. PROJECT NO.	
c.	9b. OTHER REPORT NO(S) *(Any other numbers that may be assigned this report)*
d.	

10. AVAILABILITY/LIMITATION NOTICES

Qualified requestors may obtain copies of this report from DDC.

11. SUPPLEMENTARY NOTES	12. SPONSORING MILITARY ACTIVITY
	Office of Naval Research Washington, D. C.

13. ABSTRACT

This report covers a research project administered under the JANAIR Program to investigate the feasibility of using the main rotor blade of a helicopter as a high resolution radar antenna. The purpose of this program conducted by Bell Helicopter Company with David W. Young and Associates, Inc. as a major subcontractor was to refine the design developed under Phase I of Contract Number Nonr 4148(00), documented in Bell Helicopter Company Report No. 299-099-251. Fifteen-inch antenna sections were built and tested to study detailed leading and trailing edge array element environments. A full length, 173-inch array was built and tested. A jig was constructed to accept the full length array, and radiation pattern measurements made of beamwidth, focus, sidelobe levels, and front-to-back ratios. Beamwidth and sidelobes were measured under deflections simulating maximum flight loads. Photographs of thin radar sector slices emphasizing elevation and azimuth obstacle sensing capabilities taken from a modified PPI were compared with optical photographs. The array was then installed, covered with an erosion boot and tested in the leading edge of a used UH-1B rotor blade.

DD FORM 1 JAN 64 1473

Unclassified

Security Classification

14. KEY WORDS	LINK A		LINK B		LINK C	
	ROLE	WT	ROLE	WT	ROLE	WT
Helicopter Main Rotor Blade Radar Antenna						

INSTRUCTIONS

1. ORIGINATING ACTIVITY: Enter the name and address of the contractor, subcontractor, grantee, Department of Defense activity or other organization *(corporate author)* issuing the report.

2a. REPORT SECURITY CLASSIFICATION: Enter the overall security classification of the report. Indicate whether "Restricted Data" is included. Marking is to be in accordance with appropriate security regulations.

2b. GROUP: Automatic downgrading is specified in DoD Directive 5200.10 and Armed Forces Industrial Manual. Enter the group number. Also, when applicable, show that optional markings have been used for Group 3 and Group 4 as authorized.

3. REPORT TITLE: Enter the complete report title in all capital letters. Titles in all cases should be unclassified. If a meaningful title cannot be selected without classification, show title classification in all capitals in parenthesis immediately following the title.

4. DESCRIPTIVE NOTES: If appropriate, enter the type of report, e.g., interim, progress, summary, annual, or final. Give the inclusive dates when a specific reporting period is covered.

5. AUTHOR(S): Enter the name(s) of author(s) as shown on or in the report. Enter last name, first name, middle initial. If military, show rank and branch of service. The name of the principal author is an absolute minimum requirement.

6. REPORT DATE: Enter the date of the report as day, month, year; or month, year. If more than one date appears on the report, use date of publication.

7a. TOTAL NUMBER OF PAGES: The total page count should follow normal pagination procedures, i.e., enter the number of pages containing information.

7b. NUMBER OF REFERENCES: Enter the total number of references cited in the report.

8a. CONTRACT OR GRANT NUMBER: If appropriate, enter the applicable number of the contract or grant under which the report was written.

8b, 8c, & 8d. PROJECT NUMBER: Enter the appropriate military department identification, such as project number, subproject number, system numbers, task number, etc.

9a. ORIGINATOR'S REPORT NUMBER(S): Enter the official report number by which the document will be identified and controlled by the originating activity. This number must be unique to this report.

9b. OTHER REPORT NUMBER(S): If the report has been assigned any other report numbers *(either by the originator or by the sponsor)*, also enter this number(s).

10. AVAILABILITY/LIMITATION NOTICES: Enter any limitations on further dissemination of the report, other than those imposed by security classification, using standard statements such as:

(1) "Qualified requesters may obtain copies of this report from DDC."

(2) "Foreign announcement and dissemination of this report by DDC is not authorized."

(3) "U. S. Government agencies may obtain copies of this report directly from DDC. Other qualified DDC users shall request through _____."

(4) "U. S. military agencies may obtain copies of this report directly from DDC. Other qualified users shall request through _____."

(5) "All distribution of this report is controlled. Qualified DDC users shall request through _____."

If the report has been furnished to the Office of Technical Services, Department of Commerce, for sale to the public, indicate this fact and enter the price, if known.

11. SUPPLEMENTARY NOTES: Use for additional explanatory notes.

12. SPONSORING MILITARY ACTIVITY: Enter the name of the departmental project office or laboratory sponsoring *(paying for)* the research and development. Include address.

13. ABSTRACT: Enter an abstract giving a brief and factual summary of the document indicative of the report, even though it may also appear elsewhere in the body of the technical report. If additional space is required, a continuation sheet shall be attached.

It is highly desirable that the abstract of classified reports be unclassified. Each paragraph of the abstract shall end with an indication of the military security classification of the information in the paragraph, represented as *(TS), (S), (C), or (U)*.

There is no limitation on the length of the abstract. However, the suggested length is from 150 to 225 words.

14. KEY WORDS: Key words are technically meaningful terms or short phrases that characterize a report and may be used as index entries for cataloging the report. Key words must be selected so that no security classification is required. Identifiers, such as equipment model designation, trade name, military project code name, geographic location, may be used as key words but will be followed by an indication of technical context. The assignment of links, roles, and weights is optional.